

Alma Mater Studiorum Università di Bologna
Archivio istituzionale della ricerca

It's elemental, my dear watson: Validating seasonal patterns in otolith chemical chronologies

This is the final peer-reviewed author's accepted manuscript (postprint) of the following publication:

Published Version:

Hussy K., Kruger-Johnsen M., Thomsen T.B., Heredia B.D., Naeraa T., Limburg K.E., et al. (2021). It's elemental, my dear watson: Validating seasonal patterns in otolith chemical chronologies. CANADIAN JOURNAL OF FISHERIES AND AQUATIC SCIENCES, 78(5), 551-566 [10.1139/cjfas-2020-0388].

Availability:

This version is available at: <https://hdl.handle.net/11585/830214> since: 2021-08-24

Published:

DOI: <http://doi.org/10.1139/cjfas-2020-0388>

Terms of use:

Some rights reserved. The terms and conditions for the reuse of this version of the manuscript are specified in the publishing policy. For all terms of use and more information see the publisher's website.

This item was downloaded from IRIS Università di Bologna (<https://cris.unibo.it/>).
When citing, please refer to the published version.

(Article begins on next page)

This is the final peer-reviewed accepted manuscript of:

Hussy K.; Kruger-Johnsen M.; Thomsen T.B.; Heredia B.D.; Naeraa T.; Limburg K.E.; Heimbrand Y.; McQueen K.; Haase S.; Krumme U.; Casini M.; Mion M.; Radtke K.: *It's elemental, my dear watson: Validating seasonal patterns in otolith chemical chronologies*

CANADIAN JOURNAL OF FISHERIES AND AQUATIC SCIENCES VOL. 78
ISSN 0706-652X

DOI: 10.1139/cjfas-2020-0388

The final published version is available online at: <https://dx.doi.org/10.1139/cjfas-2020-0388>

Terms of use:

Some rights reserved. The terms and conditions for the reuse of this version of the manuscript are specified in the publishing policy. For all terms of use and more information see the publisher's website.

This item was downloaded from IRIS Università di Bologna (<https://cris.unibo.it/>)

When citing, please refer to the published version.

Title: It's elemental, my dear Watson: validating seasonal patterns in otolith chemical chronologies

Authors

Karin Hüssy^{1*}, Maria Krüger-Johnsen¹, Tonny Bernt Thomsen², Benjamin Dominguez Heredia², Tomas Naeraa³, Karin E. Limburg^{4,5}, Yvette Heimbrand⁵, Kate McQueen⁶, Stefanie Haase⁶, Uwe Krumme⁶, Michele Casini^{5,7}, Monica Mion⁵, Krzysztof Radtke⁸

Affiliations

¹ National Institute of Aquatic Resources, Technical University of Denmark, Kemitorvet, DK-2800 Kgs. Lyngby, Denmark

² Geological Survey of Denmark and Greenland, Øster Voldgade 10, DK-1350 Copenhagen K., Denmark

³ Lund University, Department of Geology, Sölvegatan 12, SE-22362 Lund, Sweden

⁴ State University of New York College of Environmental Science and Forestry, Syracuse, NY 13210, USA

⁵ Department of Aquatic Resources, Institute of Marine Research, Swedish University of Agricultural Sciences, Turistgatan 5, SE-453 30 Lysekil, Sweden

⁶ Thünen Institute of Baltic Sea Fisheries, Alter Hafen Süd 2, D-18069 Rostock, Germany

⁷ Department of Biological, Geological and Environmental Sciences, University of Bologna, Via Selmi 3, IT-40126 Bologna, Italy

⁸ National Marine Fisheries Research Institute, Ul. Kołłątaja 1, 81-332 Gdynia, Poland

* Corresponding author: kh@aqua.dtu.dk, Mobile +45 93511840

24

25 Competing interests: The authors declare there are no competing interests.

26

27

Abstract

Accurate age data is essential for reliable fish stock assessment. Yet many stocks suffer from inconsistencies in age interpretation. A new approach to obtain age makes use of the chemical composition of otoliths. This study validates the periodicity of recurrent patterns in ^{25}Mg , ^{31}P , ^{34}K , ^{55}Mn , ^{63}Cu , ^{64}Zn , ^{66}Zn , ^{85}Rb , ^{88}Sr , ^{138}Ba , and ^{208}Pb in Baltic cod (*Gadus morhua*) otoliths from tag-recapture and known-age samples. Otolith P concentrations showed the highest consistency in seasonality over the years, with minima co-occurring with otolith winter zones in the known-age otoliths and in late winter/early spring when water temperatures are coldest in tagged cod. The timing of minima differs between stocks, occurring around February in western Baltic cod and one month later in eastern Baltic cod; seasonal maxima are also stock-specific, occurring in August and October, respectively. The amplitude in P is larger in faster-growing western compared to eastern Baltic cod. Seasonal patterns with minima in winter/late spring were also evident in Mg and Mn, but less consistent over time and fish size than P. Chronological patterns in P, and to a lesser extent Mg and Mn, may have the potential to supplement traditional age estimation or to guide the visual identification of translucent and opaque otolith patterns used in traditional age estimation.

Key words

Age validation, elements, microchemistry, otolith, physiology, seasonal patterns

Introduction

Age information is one of the basic input variables in modern stock assessments, from which parameters such as growth, maturation patterns and productivity are estimated. Accurate age estimates are thus crucial for reliable stock assessment and sustainable management of fish stocks. Age has traditionally been determined by counting seasonally recurring growth zones in the fish's otoliths (Campana, 2001). In temperate species, the timing of zone formation in otoliths is generally linked with seasonal cycles, particularly in temperature, leading to clearly defined growth zones and annuli (Beckman and Wilson, 1995; Høie and Folkvord, 2006; Weidman and Millner, 2000). Due to the key role of age in stock assessment models, inconsistencies in the age estimates between readers can fundamentally influence the accuracy of the stock assessment. Previously, to validate the accuracy of age estimates and/or the seasonality of growth zone formation, a suite of methods has been used – see review in Campana (2001). Methods validating the seasonality of zone formation indirectly include marginal increment analysis, date-specific natural markers and length mode progression, while tag-recapture of chemically tagged fish is the best-known direct method. In terms of validating absolute fish age, methods such as numerical integration of daily increments, bomb radiocarbon and radiochemical dating are available (Campana, 2001).

A new promising approach as a tool to validate zone formation, or even estimate absolute age, makes use of the otolith chronological chemical composition. Interest in the chemical composition, often termed “microchemistry”, of otoliths has been increasing steadily over the last two decades (see reviews in Campana (1999) and Sturrock et al. (2012)). The primary focus of these studies has been the reconstruction of environmental exposure, notably the use of strontium (Sr), barium (Ba) and manganese (Mn) to infer migrations between areas with different salinities (Kraus and

Secor, 2004; Sturrock et al., 2012) or hypoxia exposure (Altenritter and Walther, 2019; Limburg et al., 2011; Mohan and Walther, 2016) and other elements as tracers of anthropogenic contamination (Ranaldi and Gagnon, 2008). Elements that are under physiological control, such as phosphorus (P) and zinc (Zn), on the other hand, have received far less attention (Campana, 1999). Seasonality in fish growth seems to be reflected in some of these elements. In a range of species, otolith Zn correlates with visually-identified seasonal growth zones, with minimum Zn concentrations occurring within translucent winter zones with visibly reduced daily growth rings and check marks (Friedrich and Halden, 2010; Halden and Friedrich, 2008; Halden et al., 2000; Limburg and Elfman, 2010). Higher otolith Sr levels have been observed instead to occur in opaque zones in Atlantic Bluefin tuna (*Thunnus thynnus*) (Siskey et al., 2016), with inverse patterns in sodium (Na) and potassium (K) (Seyama et al., 1991) – while Tomás et al. (2006) observed higher Sr and lower Na in translucent zones in European hake (*Merluccius merluccius*). Only recently has the use of seasonal patterns in the incorporation of elements under physiological control been suggested as an alternative method to derive fish age (Hüssy et al., 2016; Limburg et al., 2018). In a comparative age estimation approach on eastern Baltic cod (*Gadus morhua*), the first study of this kind, “visual” age readers with several decades’ experience in traditional age interpretation achieved far lower precision than “microchemistry-based” age readers (Heimbrand et al., 2020), despite the fact that the latter had no formal manual to guide their interpretations. In this exercise, magnesium (Mg), and phosphorus (P) in particular, proved promising to be used as chemical clocks. However, to date no rigorous validation of such seasonality in element incorporation has been provided for any stock.

The present study aims at providing the first validation of the microchemistry-based age estimation approach, focusing on eastern Baltic cod. The eastern Baltic cod stock is a good case study, in that

93 this stock is well known for its long-lasting issues with problematic traditional age readings
94 (Berner, 1968; Hüsey et al., 2016; ICES, 2015). The ageing issues eventually resulted in a
95 discontinuation of the traditional age-based stock assessment (Eero et al., 2015; ICES, 2014). Age
96 estimation in this stock is so difficult because the contrast between seasonal growth zones is very
97 small. This lack in contrast is primarily related to a combination of the hydrographic conditions
98 prevailing in the Baltic Sea proper, coupled with the movements of the cod through complex
99 thermal and salinity gradients (Baranova et al., 2011; Hüsey et al., 2010; Hüsey, 2010; Hüsey et
100 al., 2009; Hüsey et al., 2016). Additionally, suitable samples with known age derived from analysis
101 of daily increment analysis (DECODE, 2009; Hüsey et al., 2010; Hüsey et al., 2018) and a tag-
102 recapture program with chemically tagged otoliths from the “Tagging Baltic cod” project
103 (TABACOD, <http://www.tabacod.dtu.dk/>) are available (Hüsey et al. 2020a).

104 The trace element composition of otoliths depends on specific mechanisms of incorporation during
105 the biomineralisation process. Elements either substitute for calcium (Ca) in the growing calcium
106 carbonate (CaCO_3) crystals, are randomly trapped in the interstitial spaces between crystals, or are
107 bound as co-factors in the organic matrix that provides the scaffolding for otolith crystal growth.
108 Sr and Ba are known to substitute for Ca, while Mg, K and Pb are randomly trapped (Doubleday
109 et al., 2014; Izzo et al., 2016; Miller et al., 2006; Thomas et al., 2017). These elements therefore
110 reflect environmental concentrations. P, Cu and Zn on the other hand are co-factors in enzymes
111 involved in biomineralisation of the otoliths, or active transport of carbonate across the
112 endolymphatic epithelium (Borelli et al., 2003; Payan et al., 2004), and are thus under strong
113 physiological control. Recent evidence suggests that Mn and Mg appear to occur in both crystal
114 and organic fraction of the otolith (Izzo et al., 2016; Thomas et al., 2017; Thomas and Swearer,
115 2019) and therefore presumably are under both environmental and physiological control (Hüsey et

116 al., 2020b). Elements that substitute for Ca (elements of similar size and charge as Ca), or are
117 randomly trapped in the CaCO_3 crystal lattice, should therefore reflect ambient environmental
118 conditions in a consistent and predictable manner (Campana, 1999; Hüsey et al., 2020b), while
119 matrix-bound elements should be regulated by physiological processes (Limburg et al., 2018;
120 Hüsey et al., 2020b), reflecting seasonal variations in growth.

121 Based on the respective incorporation mechanisms of different elements, the objectives of this
122 study are to test the hypotheses that i) only elements under physiological control exhibit annually
123 recurring patterns in incorporation, linked to seasonal variations in environment and/or fish
124 physiology, ii) element incorporation is lowest during the coldest time of the year, iii) the number
125 of minima in element concentration corresponds to the fish's true age. Additional objectives of
126 this study are iv) to explore stock-related differences in element patterns, and v) to identify
127 elements that are most suited for age determination.

128 **Materials and methods**

129 **Samples**

130 The otoliths used in this study are from three different collections: one “test” collection and two
131 “validation” collections.

132 *Test collection (TEST):* This collection consists of 40 cod otoliths collected in the Kattegat (ICES
133 SD 21, see Fig. 1 for details on areas and sample locations) in December 2016. Otoliths from the
134 Kattegat are characterized by high contrast between seasonal translucent and opaque zones with
135 concurrent high age estimation precision and well established ageing protocols. These samples are
136 used as test group to identify the best approach for the analyses of element profiles. Details of cod
137 size and age are shown in Table 1.

139 *Validation collection 1 (DECODE)*: This collection consists of 53 otoliths from Baltic cod in the
140 size range 150 – 350 mm captured in the Bornholm Basin (ICES SD 25) in February of 2001 and
141 2004 (Fig. 1, Table 1). In the otoliths of these cod, patterns in daily increments have previously
142 been analysed in the DECODE project (DECODE, 2009). The DECODE project made use of a
143 technique to estimate the age of young fish based on the width of daily otolith growth increments
144 and has previously been used to identify problems with traditional age estimation (Hüsey, 2010)
145 as well as to estimate changes in growth patterns (Hüsey et al., 2018). The width of daily growth
146 increments is linked to the annual cycle in environmental temperature experienced by the cod
147 (Hüsey et al., 2010). This results in distinct patterns where periods with clearly discernible
148 increments formed during summer are interrupted by zones without regular increment structure
149 during winter (DECODE, 2009; Hüsey et al., 2010). Counting these zones without increments thus
150 provides an estimate of the fish's age, while their distance to the core provides a time stamp
151 identifying the coldest time of the year the fish had experienced. These samples thus provide the
152 means to validate both seasonality in element pattern formation as well as absolute age of the fish.

153 *Validation collection 2 (TABACOD)*: This collection consists of otoliths from the tag-recapture
154 program “Tagging Baltic Cod” – TABACOD – carried out in the Baltic Sea. See Hüsey et al.
155 (2020a) for details on tagging protocols, including release and recapture statistics. Tagged cod
156 were > 250 mm at release and were marked externally using T-bar tags with a unique number
157 identifying each fish throughout the years 2016 – 2019 (<http://www.tabacod.dtu.dk/>) (Fig. 1).
158 Otoliths were marked with an injection of tetracycline-hydrochloride (TET), leaving a fluorescent
159 mark in the otolith when viewed under UV light. Cod were tagged in the western (ICES SD 24)
160 and eastern (ICES SDs 25 and 26) Baltic Sea. Stock identity of the recaptures was determined
161 using a combination of genotyping and otolith shape based methods, the details of which are

described in Hemmer-Hansen et al. (2019) and Schade et al. (2019). Days at liberty (*DAL*) were defined as the days between release of tagged cod and recapture. Since tagging was primarily carried out in spring and fall (Hüssy et al., 2020a), the samples used in this study were restricted to fish with *DAL* > 180 in order to ensure temporal overlap of individuals across all seasons in all years. A total of 143 recaptured cod (123 eastern and 20 western) in the length range 177 – 500 mm were available. For details on length and *DAL* between tagging and recapture, see Table 1 and Supplementary Fig. S1. These recaptures thus allow testing for annually recurring patterns in element composition without the need to count daily increments. The tagging experiments were conducted under the following national animal test permissions; Germany: AZ 7221.3.1-029/15; Denmark: 016-15-0201-00929, Poland: no 19/2016, dated 28.06.2016, Sweden: Dnr 5.8.18-14823/2018.

Otolith preparation

For the *TEST* and the *TABACOD* samples, otoliths were soaked in deionized water, cleaned for 10 minutes in an ultrasonic bath of deionized water, rinsed under deionized water and left to dry overnight under a laminar flow hood in acid-washed trays. Otoliths were embedded in Epoxy resin (Struers®) and sectioned through the core using an Accutom-100 multi-cut sectioning machine to obtain a 10 mm wide block containing the rostral part of the otolith with the nucleus exposed at the sectioned surface. The surface of each section was polished with 3 µm abrasive paper mounted on rotating disks (Buehler®) to obtain a smooth surface and cleaned in the ultrasonic bath again as described above. Otolith sections were digitized using a Leica DCF290 camera at a magnification of 380 µm pixel⁻¹ with a standard setup (8 bit/channel, 2048 x 1536 pixel frame).

184 For the *TEST* images, otolith translucent seasonal growth zones (*TZ*) were identified and counted.
 185 The number of *TZ* is assumed to correspond to the age of the fish (Fig. 2).
 186 For the *DECODE* samples, otolith preparation and imaging was similar to the above samples (for
 187 detailed description see: Hüsey et al., 2010; Hüsey, 2010; Hüsey et al., 2018). For these otoliths,
 188 measurements of the distance from the core to the middle of each successive winter growth zone
 189 (*WZ*) along the dorsal growth axis were measured using ImageJ (Rueden et al., 2017), representing
 190 a chronological age record of each fish (Fig. 3). Each individual element measurement (see below)
 191 was assigned to the chronological age of formation in relation to the *WZ*. It is important to note
 192 that all individuals were sampled in February. Since this is just prior to the coldest time of the year
 193 (occurring in March), daily increment analysis was not able to fully capture the last *WZ*, as this is
 194 just forming at the otolith edge. By definition, the “birthday” of fish is the 1st January, and for fish
 195 caught after this date, the edge is also counted when ageing the fish. In the present case, the age of
 196 the fish therefore is the number of complete *WZ* +1.
 197 The *TABACOD* otoliths were viewed under UV light using a Leica DMLB microscope (with a BP
 198 355-425 excitation filter, magnification of 1.36 $\mu\text{m pixel}^{-1}$, 3,648 x 2,736 pixel frame) (Fig. 4).
 199 The distance from the TET mark to the otolith edge was measured along the dorsal axis together
 200 with the total axis length from core to edge. Otolith growth (G_{oto}) from TET mark to the otolith
 201 edge was linearly correlated with days at liberty (*DAL*) (eastern: $G_{\text{oto}} = 1.203 \cdot \text{DAL}$, $\text{df} = 255$, r^2
 202 $= 0.74$, $p < 0.05$; western: $G_{\text{oto}} = 1.880 \cdot \text{DAL}$, $\text{df} = 40$, $r^2 = 0.82$, $p < 0.05$). Otolith growth during
 203 the tagging period was thus approximately constant throughout the year. Each individual element
 204 measurement (see below) was assigned to a date of formation calculated from its distance to the
 205 TET mark and the proportional relationship between *DAL* and G_{oto} .

207 Microchemistry

208 For the *TEST* and *TABACOD* samples, trace element analyses were carried out by Laser Ablation
209 Inductively Coupled Plasma Mass Spectrometry (LA-ICP-MS) at the Geological Survey of
210 Denmark and Greenland (GEUS), employing a NWR213 frequency-quintupled Nd:YAG solid
211 state laser system from Elemental Scientific Lasers (ESI) that was coupled to an ELEMENT 2
212 double-focusing, single-collector magnetic sector field ICP-MS from Thermo-Fisher Scientific.
213 Each transect line analysis used a beam diameter of 40 μm and a laser fluence of $\sim 9.5 \text{ J/cm}^2$, a
214 repetition rate of 10 Hz, and a travelling speed of 5 $\mu\text{m sec}^{-1}$. This study focused on the
215 measurement of magnesium (^{25}Mg), phosphorus (^{31}P), calcium (^{43}Ca), manganese (^{55}Mn), copper
216 (^{65}Cu), zinc (^{66}Zn), strontium (^{88}Sr) and barium (^{137}Ba). For a complete overview of analytical
217 settings, see Table S1a.

218 The *DECODE* collection was analysed at the Department of Geology at Lund University,
219 employing a Teledyne Photon Machines G2 excimer laser coupled to a Bruker Aurora Elite
220 quadrupole ICP-MS. The laser equipped with a HelEx 2-volume sample cell. Instrument tuning
221 was done using the NIST612 glass standard, opting for high sensitivity and stable signal counts on
222 relevant isotopes, and for a low oxide production (i.e. below 0.5 %). The analyses were set to run
223 automatically using a standard-sample bracketing and with pre-ablation prior to each transect
224 analyses. The background level was measured for 30 seconds before each measurement. Transect
225 line analysis used a scan speed of 12 $\mu\text{m sec}^{-1}$, circular spots, and laser repetition rate of 7 Hz and
226 a fluence of 2 J cm^{-2} on the carbonate phases and 3 J cm^{-2} on the NIST glass. The following isotopes
227 were measured: ^{25}Mg , ^{31}P , ^{43}Ca , ^{55}Mn , ^{63}Cu , ^{64}Zn , ^{66}Zn , ^{85}Rb , ^{88}Sr , ^{138}Ba , ^{208}Pb . For a complete
228 overview of analytical settings, see Table S1b.

Concentrations in all collections are reported as element:Ca ratios in ppm, using ^{43}Ca as an internal standard element and calibrated to a Ca concentration of 38.3 wt. % to account for any parameters affecting the ablation yield, such as plasma fluctuations and variation in the amount of ablated material. Further details on operating conditions, data acquisition parameters, analytical protocols and data processing techniques are described in Supplementary Table S1a and S1b and Serre et al. (2018). In the following, element will be called by their abbreviations without their mass number. The otoliths were analysed along a transect from the nucleus to the dorsal edge of the otolith following the axis of maximum growth. The data thus represent elemental signatures spanning from hatch to death of each individual. Values $> 4\times$ standard deviations from the transect mean were treated as outliers and discarded. For Mg, Mn, P, Sr and Ba less than 1% outliers were removed, for Cu and Zn 10 – 20% were considered outliers. Signal to noise ratios (μ^2/s^2), where μ and s are the mean and variance of measurements respectively were < 5 in Cu and Zn in most individual owing to the fact that their concentration is close to the analytical resolution threshold (Serre et al., 2018). The results of these elements are shown with the others, but results are to be treated with caution.

Statistical analyses

Peak detection: A standardised method for identifying extrema (minima and maxima) in the elemental profiles was developed by first smoothing the profiles with local polynomial regression “loess” in “R” (R Development Core Team, 2020). Local extrema, maxima *Max* and minima *Min* were then identified with the “peaks” function, where a peak/valley is defined as the measurement in a sequence which is greater/smaller than all other measurements within a window of width span centred at that measurement (Constantine, 2007). Successful extremum identification depends on

the correct settings of the algorithm. The optimal settings of the *TEST* sample were identified using the profiles of P and Mg, the most promising elements for age estimation (Heimbrand et al., 2020). Combinations of settings were tested until the approach identified the maximum correspondence in number of *Min* as the corresponding number of *TZ* (Fig. 2). The distribution of the resulting differences in *TZ - Min*, of the P profiles show a consistent difference of one (Supplementary Fig. S2), because the last *Min* in most samples was too close to the edge to be captured by any algorithm settings (see Supplementary Fig. S3 for explanation). Laser scan speed and subsequent data treatment differed between the two LA-ICP-MS facilities, designed to optimize data precision of the respective instruments. The impact of these settings (*TEST* and *TABACOD* samples: 5 $\mu\text{m s}^{-1}$, averaging 4 consecutive measurements; *DECODE* samples: 12 $\mu\text{m s}^{-1}$, all measurements are reported) was assessed, but no impact on extrema detection was found (see Supplementary Fig. S4 for explanation). The optimal settings identified were: “loess” with span (degree of smoothing) = 0.3 and degree of polynomials = 2, and “peaks” with span (minimum distance for peaks have to be counted) = 151 and without threshold value.

Validation 1 (DECODE): In the *DECODE* otoliths, element concentrations were analysed as a function of distance to the core using the smoothing algorithm and minimum detection routine defined from the *TEST* sample. Along the profile of all elements, the distance of each minimum (*Min*) to the core was recorded, as well as the loess estimate at each *Min*. The extent to which the distances from core to *Min* of an element co-occurred with *WZ* from daily increment patterns was assessed using a Linear Mixed Effects Model (LME) with *Min* as response variable, *WZ* as fixed effect and minima within individual fish as random effects.

Validation 2 (TABACOD): Ideally, data of recaptures with *DAL* > 360 and from different years should be used for validating seasonality with tag-recapture data. Only few fish fulfil that

requirement (Fig. S1). To mitigate for this shortcoming, data from all fish were pooled and treated as a single-fish analysis. If there are identifiable patterns in such an approach, these are the result of true seasonal variation in element incorporation across individuals and years. Without a consistent seasonal element incorporation, the result would consist exclusively of noise. Element concentrations typically show high inter-individual variation. In order to remove this variation, relative element concentrations were calculated by dividing each measurement with the mean value of all measurements from TET mark to otolith edge. Relative element concentrations were then analysed as a function of date of formation using all measurement of all otoliths in the sample, regardless of how many days at liberty they had. This dataset was then smoothed and *Min* as well as *Max* identified with the loess smoothing algorithm and peak detection routine defined from the *TEST* sample. These analyses were carried out on individuals from the eastern and western stocks separately.

Results

Validation 1: *DECODE* samples

For cod < 350 mm, the correspondence between daily increment patterns and *Min* in element signals was analysed. An example of profiles of each analysed element in relation to distance from the core is shown for a 4-year old cod in Fig. 5. The analysis of correspondence between daily increment patterns and element signals, shows that the distance of elemental *Min* is linearly related with the corresponding winter zones *WZ* (Fig. 6). Statistics of each correlation are summarized in Table 2. An intercept of 0 and slope of 1 would be expected if *Min* and *WZ* corresponded directly. A *Min* formation before *WZ* would result in a negative intercept, formation after *WZ* in a positive intercept, while the intercept would not be statistically significant if the two co-occurred. However,

both these values are not contained within the confidence intervals of any of the elements (Table 2), where all intercepts are significantly larger than 0 and all slopes differ significantly from 1 (LME, all $p < 0.05$). This suggests that minima in element patterns occur after the middle of the winter zone identified from daily increment widths. Lowest correlation coefficients occur for the environmentally regulated elements Sr and Ba (both $r^2 \leq 0.60$), while the elements under physiological control – notably P and Zn – show the highest correlation coefficients (both ≥ 0.74). Also Zn, Pb and the two elements under environmental and physiological control, Mg and Mn, have correlation coefficients of $r^2 \geq 0.62$. By far the strongest correlation between *Min* and *WZ* is found in P ($r^2 = 0.80$). These results show that in cod < 350 mm, in particular P provides accurate age estimates, followed by Mg and Zn.

In order to explore the variability in these regressions further, histograms of known age derived from daily increment patterns minus the number of element minima (*WZ* – *Min*) were examined (Fig. 7). These histograms show that the highest proportion of correct age estimates were obtained by the physiologically regulated elements Cu (51%), P (49%) and Mg (43%) Zn (47%) – and the environmentally regulated Sr (55%). The combined results of the two analyses (Table 2, Fig. 7) thus show that Sr provides the estimate with the highest accuracy (55%), but with a much lower precision ($r^2 = 0.57$) compared to P (accuracy 49%, $r^2 = 0.81$) and Mg (accuracy 43%, $r^2 = 0.73$). For P, the chemical method underestimates age by 1 year in a considerable proportion of individuals (31%), while a smaller proportion of ages are overestimated. Visual inspection of element profiles and the locations of *WZ* and *Min* found that these discrepancies were largely attributable to the smoothing and extremum detection functions used, more specifically their lack of ability to identify *Min* close to the end of the profile at the otolith edge. Including this additional *Min* at the otolith edge manually in the total *Min* number, resulted in considerably higher

321 accuracies: P – 80%, Mg – 81%, Sr – 77%. Underestimation was thus primarily associated with
322 insufficient minima detection close to the otolith edge, while overestimation occurred in profiles
323 with evident sub-seasonal profile patterns (Fig. S3).

324 325 Validation 2: *TABACOD* samples

326 For tagged cod > 250 mm minima and maxima in element signals were identified in order to
327 identify generic patterns in extrema formation. In Fig. 8 the individual with the longest time at
328 liberty (*DAL* = 927 days) is shown as an example. The element profiles from TET mark to the
329 otolith edge of this individual are typical for eastern Baltic *TABACOD* cod. Combining all profiles
330 of fish with *DAL* > 180 days, the relative element concentrations in relation to date of formation
331 show conspicuous differences between elements and stocks, which mirrors those of Fig. 8.
332 Elements under environmental control (Fig. 9) show moderate (Sr) to low (Ba, K) seasonal patterns
333 with minima in summer and maxima in winter in eastern Baltic cod, while variations in the
334 concentration of these elements seem random in western Baltic cod. In the elements under both
335 environmental and physiological control (Fig. 10), Mn and Mg, on the other hand show clear and
336 highly consistent seasonal patterns in incorporation in both stocks.

337 In the elements under physiological control (Cu, P, Zn,) (Fig. 11), phosphorus in particular exhibits
338 strong seasonal patterns where *Min* and *Max* occur consistently at approximately 12-month
339 intervals across all years in both stocks, but with stock-specific timing in extremum formation. In
340 eastern Baltic cod, minima are formed in March and maxima around October, while for western
341 Baltic cod, minima are formed around February and maxima in September/October. These patterns
342 are mirrored in Mn (with the exception of an additional minimum in WBC), and Mg. Notably, the

amplitude between *Min* and subsequent *Max* is larger in western than eastern Baltic cod, resulting in more pronounced seasonal signals (Fig. 11).

Discussion

The concept of using otolith chemical composition for age estimation is in its infancy (Hüssy et al., 2016; Limburg et al., 2018) originating from decades of severe issues in age estimation of Baltic cod. Heimbrand et al. (2020) hypothesized that chronological patterns in specific elements, in particular Mg and P, may be used for age estimation in fish. The present study is the first of its kind, providing validation of this hypothesis that certain chemical elements are in fact incorporated into the otolith in an annually recurring pattern which would make them useful as tool for age estimation. We provided evidence that the chronological records of otolith P concentrations showed the highest consistency in seasonal variation over the years, with minima occurring in late winter/early spring when water temperatures are coldest and a seasonal amplitude which is considerably larger in western compared to eastern Baltic cod. In the following we will highlight differences in chronological patterns between elements with different incorporation mechanisms, discuss these patterns in the context of stock-specific environmental conditions and the elements usefulness for age determination.

Seasonality in element patterns

Elements reflecting environmental concentrations - Sr Ba, Pb and K - do not show strong, consistent seasonal patterns across fish sizes (reflected in both *DECODE* and *TABACOD* otoliths) and stocks, with two exceptions: Pb in *DECODE* and Sr in *TABACOD* otoliths. In *DECODE* otoliths, increases in Pb in summer may be attributable to the juvenile cod's shallower vertical

366 distribution (Oeberst, 2008; Pihl, 1982; Pihl and Ulmestrand, 1993) with associated high
367 consumption of benthic crustaceans (Hüssy et al., 1997) that exhibit seasonal patterns in Pb, as
368 well as Cu and Zn (Swaileh and Adelung, 1995). In eastern *TABACOD* cod, there are nevertheless
369 weak signals that seemingly correspond to seasonal patterns in Sr. Evidence from a range of
370 species suggests that seasonal peaks in otolith Sr coincides with peak spawning (Clarke and
371 Friedland, 2004; Granzotto et al., 2003; Kalish, 1991; Sturrock et al., 2015) reflecting a change in
372 Sr availability in the blood plasma (Sturrock et al., 2015). However, in this study highest Sr
373 concentrations occur during winter, while the peak spawning time of eastern Baltic cod is in July
374 – August (Bleil et al., 2009; Wieland et al., 2000). The seasonal pattern in Sr can therefore not be
375 attributed to spawning as such. Given the Baltic Seas vertical stratification, where bottom water
376 has a much higher salinity, seasonal migrations may contribute to a seasonal signal in otolith Sr
377 concentration. Overall this study supports the hypothesis that elements that co-vary with
378 environmental concentration are generally not useful for age estimation, at least for Baltic cod.

379 Among the elements regulated by physiological processes, P varies consistently over the seasons
380 in both validation samples with minima co-occurring with otolith zones without visible daily
381 increments in *DECODE* otoliths or, in the case of the *TABACOD* otoliths, in late winter/early
382 spring. The amplitude in P is considerably larger in western compared to eastern Baltic cod
383 corresponding to known stock-specific differences in growth rate (Bagge et al., 1994; McQueen
384 et al., 2020) and experienced temperature amplitude, apparently with a smaller variation around
385 the mean values in the western Baltic cod. Throughout the Baltic Sea, phosphate concentrations
386 are low from April to September, presumably owing to a combination of increased primary
387 production (Wulff and Rahm, 1988) coupled with a precipitation-related increase in P loading
388 during fall/winter (Rolff et al., 2008) and recycling in the sediments in hypoxic areas (Viktorsson

et al., 2013). The seasonal bio-availability of phosphorus in the environment is thus out of phase with the P concentrations observed in the otoliths. P does therefore indeed seem to be a consistent tracer of seasonally varying physiological activity and growth rates in Baltic cod. In Cu and Zn, element minima also co-occur with winter zones in individual *DECODE* otoliths – but these signals disappear when profiles of fish are combined suggesting some variation in the timing of minima among individuals. In *TABACOD* otoliths, there seems to be no relation between minima and time of the year either. This lack in seasonality in Baltic cod may be related to family-specific incorporation mechanism, in that no such patterns occur in Osmeridae either (Limburg and Elfman, 2010), while Zn concentrations in families like Salmonidae and Esocidae are at a minimum in winter (Friedrich and Halden, 2010; Halden and Friedrich, 2008; Halden et al., 2000; Limburg and Elfman, 2010). Additionally, one should also bear in mind that the concentrations of these elements are very low, with low signal to noise ratios. Evidently, Cu and Zn are therefore not suitable for age estimation – at least for Baltic cod.

Seasonal signals with minima during winter/late spring are also evident in Mg and Mn for both *DECODE* and especially *TABACOD* otoliths. While element uptake in marine fish generally occurs from the water (Doubleday et al., 2013; Walther and Thorrold, 2006), dietary Mg enrichment results in increased otolith Mg (Shearer and Åsgård, 1992). There is also growing evidence that otolith Mg is tied to metabolism (Limburg et al., 2018; Thomas and Swearer, 2019). Variations in Mg therefore may represent dietary and metabolic processes. The present results support a strong physiological component, presumably related to consumption, in the incorporation of the two elements as suggested by Limburg et al. (2018) and Limburg and Casini (2018). Mg was also, together with P, identified as the element with the highest precision among age readers using chemical profiles for ageing Baltic cod, with an agreement of 74% compared to

50% for traditional ageing with coefficients of variation of 10% and 22% respectively (Heimbrand et al., 2020). Otolith Mn on the other hand, reflects environmental concentrations of Mn^{2+} made available during hypoxia, with some additional physiological regulation (Altenritter et al., 2018; Limburg and Casini, 2018; Thomas and Swearer, 2019). In the Baltic Sea, hypoxia is known to occur frequently in shallow coastal areas during summer/fall (Conley et al., 2001) in addition to the persistent hypoxia in the deeper areas of the Bornholm Basin (Viktorsson, 2017). The seasonal signals, particularly apparent in the eastern Baltic cod otoliths, seem thus to reflect exposure to higher environmental Mn concentrations during the spawning season in summer (Bleil et al., 2009; Wieland et al., 2000) spent in the deeper areas of the Bornholm Basin (Nielsen et al., 2013; Hüsey et al., 2020a). The more irregular patterns in western Baltic cod otoliths may instead reflect summer-residence in more ephemeral hypoxic areas (Funk et al., 2020).

Timing of seasonal patterns

Small, yet consistent differences between the two Baltic cod stocks are evident in the elemental minima of P, Mg and Mn in the otoliths of tagged *TABACOD* cod. In eastern Baltic cod, these minima occur in March, but in western Baltic cod somewhat earlier – in January/February. Maxima occur in October/November and August/September in western and eastern Baltic cod respectively. In the following we will examine to what extent these stock-specific differences in extremum formation are attributable to water temperature or fish growth.

Eastern Baltic cod: The coldest temperatures experienced by eastern Baltic cod occur during March and highest temperatures in October – November, as data from archival tags have shown (Hüsey et al., 2009, 2010; Righton et al., 2010; Hüsey et al., 2020a). Otolith growth modelling suggests that otolith increment formation apparently ceases at temperatures $< 5 - 6^{\circ}C$. in *DECODE*

435 otoliths (Hüssy et al., 2010), occurring in March/April at the depths inhabited by cod at that time
436 of the year. In eastern Baltic cod, the seasonal temperature experienced is reflected in fish somatic
437 growth patterns as well. A recent paper examining growth from tagging programs across multiple
438 decades (1955 – 1970), found minima and peaks in growth rates in March and September
439 respectively (Mion et al., 2020). However, a corresponding analysis with TABACOD data was not
440 able to detect seasonal variations in somatic growth (Mion et al., in review), which suggests that
441 otolith P concentration is not only a function of somatic growth.

442 *Western Baltic cod:* Cod in the western Baltic sea experience the lowest and warmest water
443 temperatures in January/February and August – October respectively (MARNET, 2020). The
444 timing of elemental extremum formation thus corresponds with the temporal temperature patterns.
445 Also in western Baltic cod historic tagging data from 1965 – 1972 found seasonally varying
446 somatic growth (Borrmann and Berner, 1983; Berner and Borrmann, 1985). Borrmann and Berner
447 (1983) attributed the difference in winter minimum to the maturation/spawning cycle. Berner and
448 Borrmann (1985) further noticed that seasonal minima in growth occurred in January in fast
449 growing cod, but first in mid-April in slow growing cod, attributing the disparity to different stock
450 origin of the tagged cod. A recent study on cod tagged on two artificial reefs in 2007-2015 found
451 minima and peaks in somatic growth to occur in May and November, respectively (McQueen *et*
452 *al.*, 2019). Both minima and peaks in growth of this stock occur approximately 3 months after the
453 corresponding element and temperature extrema. The reason for this apparent shift in timing over
454 time are somewhat unclear, but could be related to analytical differences (historic growth not
455 calculated on length change of individuals but mean sizes at estimated age), tagging of different
456 stock components (local sub-structuring of cod stocks in coastal areas of the Baltic Sea (Wenne et

al., 2020)), or a climate change driven increase in summer temperatures to above-optimal levels for cod growth.

The seasonal growth patterns from tagging studies of the eastern stock thus mirror the elemental patterns from this study very well, and support a close coupling between seasonal temperature, consumption and growth (Campana et al., 1995; Mello and Rose, 2005; Pörtner et al., 2001; Schwalme and Chouinard, 1999) and incorporation of P, Mg and Mn - where minima in elements occur when water temperatures are coldest and growth slowest. The corresponding information from the western stock on the other hand indicates that the coupling between these processes may be influenced by a range of additional, and to date unknown, factors.

Correspondence between age and number of element minima

The most basic requirement for a new age estimation method to be applicable for stocks where traditional age estimation is not possible, is that it provides age estimates that are accurate (without bias) and with high precision. In the present study, the number of chemical minima in P, Zn and Mg only corresponded with the fish's known age in approximately 45 - 50% of the samples. Under-estimation of the number of minima was largely attributable to the fact that extremum detection methods need sufficient measurements on either side of the extremum in order to be able to identify it correctly. Taking account for these missing minima at the edge of the otolith increased the correspondence between known age and chemistry-derived age to approximately 80%. One way to avoid this issue in the future would be to select otoliths sampled just after the main growth season between summer and early winter (and not at the coldest time of the year as the *DECODE* samples in this study), giving the otoliths time to add a new growth increment. Over-estimation on the other hand occurred in fish with sub-seasonal element cycles, even if these are often less

prominent compared to the true seasonal signals. It is thus clear that the selection of a single combination of settings for profile smoothing and extremum detection may lessen the accuracy of the chemical method. Particularly so in a stock with large variability in behaviour between individuals that may cause sub-seasonal patterns in temperature experience like the eastern Baltic cod (Hüssy et al., 2009; Nielsen et al., 2013). In order to obtain an individual's correct age, visual examination of the element profiles to identify potentially missing/superfluous extrema is recommended.

Conclusion and future perspective

This study has shown that among the elements that are co-factors in the organic matrix regulating biomineralisation, only P shows consistent seasonal patterns in concentration across fish size and stocks. Other elements under physiological control (Cu and Zn) occur at concentrations that are too low for reliable signal detection. Mg shows similar, albeit much weaker, patterns as P, suggesting that the physiological regulation is outweighing environmental control. Elements that substitute for Ca or that are randomly trapped in the otolith crystal lattice (Sr, Ba, K, Pb) are poor indicators of growth, and by inference, the age of the fish.

Chronological patterns in P may thus have the potential to supplant/supplement traditional age estimation or to guide the visual identification of translucent and opaque otolith patterns used in traditional age estimation. Particularly in otoliths with discrepancies in interpretation between readers such as the eastern Baltic cod, the microchemistry-based approach would improve the accuracy of age estimates.

In all elements, inter-individual variation was considerable despite the application of standardization routines. Studies that explore the environmental and/or biological drivers behind

these inter-individual variations in absolute element concentrations as well as sub-seasonal pattern formations based on targeted laboratory experiments and especially information from electronic archival tags linked with chemical composition (Morita et al., 2013) are necessary to understand the physiological processes regulating element incorporation into the otolith and to improve the reliability of microchemistry as a routine age estimation method. Heimbrand et al. (2020) highlighted that patterns of P were more pronounced in older individuals, while Mg patterns were clearer in younger fish. This suggests that sexual maturation may influence the availability of elements for incorporation into the otoliths. The present study corroborates these results, suggesting that increased focus should be given to the impact of maturation and spawning on otolith element concentrations and the impact of reduced seasonal temperature fluctuations in the future.

Otolith biomineralisation is regulated by physiological and kinetic processes that may be expected to be similar across fish taxa, with similar drivers of element incorporations (Hüssy et al., 2020b). The extent to which the proposed use of chronological seasonal patterns in otolith P concentration for age estimation is applicable to other species remains to be explored.

Acknowledgements

Thanks go to all technical staff involved in the collection and processing of samples used in this study. TABACOD tagging was carried out by staff from the National Marine Fisheries Research Institute, the Technical University of Denmark, the Swedish University of Agricultural Sciences and the Thünen Institute of Baltic Sea Fisheries. Additional thanks to Kristian Ege Nielsen for the chemical analyses of samples.

Competing interests

The authors declare there are no competing interests.

Contributors' statement

KH: Conceptualization, Formal analysis, Writing - Original Draft, Project administration, Supervision, Funding acquisition

MKJ: Methodology, Investigation, Data curation

TBT: Methodology, Data curation, Writing - Review & Editing

BDH: Methodology, Data curation, Writing - Review & Editing

TN: Methodology, Writing - Review & Editing

KEL: Conceptualization, Writing - Review & Editing, Funding acquisition

YH: Conceptualization, Writing - Review & Editing

KMQ: Investigation, Data curation, Writing - Review & Editing

SH: Investigation, Data curation, Writing - Review & Editing

UK: Investigation, Writing - Review & Editing, Funding acquisition

MC: Investigation, Writing - Review & Editing, Funding acquisition

MM: Investigation, Data curation, Writing - Review & Editing

KR: Investigation, Data curation, Writing - Review & Editing, Funding acquisition

Funding statement

This study was funded by BalticSea2020 (<http://balticsea2020.org>) through the project *Tagging Baltic Cod* (TABACOD). Financial support is also acknowledged from the Danish Ministry for Environment and Food and the European Maritime Fisheries Fond [grant No. 33113-B-17-092],

the Swedish Research Council Formas [grant No. 2015-865] and the U.S. National Science Foundation under Grant [grant No. OCE-1923965].

Data availability statement

The data upon which this study is based originate from the TABACOD project. In the Cooperation Agreement of that project it has been stated that data from TABACOD will be made publicly available 5 years after the termination of the project (31/05/2025), in order to ensure project participants sufficient time to publish ongoing work. During the 5-year embargo period, access to data may be given by contacting the corresponding author.

References

- Altenritter, M.E., and Walther, B.D. 2019. The Legacy of Hypoxia: Tracking Carryover Effects of Low Oxygen Exposure in a Demersal Fish Using Geochemical Tracers. *Trans. Am. Fish. Soc.* **148**(3): 569–583. doi:10.1002/tafs.10159.
- Altenritter, M., Cohuo, A., and Walther, B. 2018. Proportions of demersal fish exposed to sublethal hypoxia revealed by otolith chemistry. *Mar. Ecol. Prog. Ser.* **589**: 193–208. doi:10.3354/meps12469.
- Bagge, O., Thurow, F., Steffensen, E., and Bay, J. 1994. The Baltic cod. *Dana* **10**: 1–28.
- Baranova, T., Müller-Karulis, B., Sics, I., and Plikshs, M. 2011. Changes in the annual life cycle of eastern Baltic cod during 1950-2010. *ICES CM* 2011/R:10.
- Beckman, D., and Wilson, C.A. 1995. Seasonal timing of opaque zone formation in fish otoliths. *In* *Recent Developments in Fish Otolith Research*. Edited by D.H. Secor, J.M. Dean, and S.E. Campana. University of South Carolina Press, Columbia, SC. pp. 27–44.

- 572 Berner, M. 1968. Einige orientierende Untersuchungen and den Otolithen des Dorsches (*Gadus*
573 *morhua* L.) aus verschiedenen Regionen der Ostsee. Fisch. Forsch. **6**: 77–86.
- 574 Berner, M., and Borrmann, H. 1985. Zum saisonalen Längenwachstum des Dorsches der
575 Mecklenburger Bucht nach Wiederfangdaten von Markierungsexperimenten und
576 Bestandsvergleichen. Fisch. Forsch. **22**(1): 63–69.
- 577 Bleil, M., Oeberst, R., and Urrutia, P. 2009. Seasonal maturity development of Baltic cod in
578 different spawning areas: importance of the Arkona Sea for the summer spawning stock. J.
579 Appl. Ichthyol. **25**(1): 10–17. doi:10.1111/j.1439-0426.2008.01172.x.
- 580 Borelli, G., Mayer-Gostan, N., Merle, P.L., Pontual, H., Boeuf, G., Allemand, D., and Payan, P.
581 2003. Composition of Biomineral Organic Matrices with Special Emphasis on Turbot (*Psetta*
582 *maxima*) Otolith and Endolymph. Calc. Tiss. Int. **72**(6): 717–725. doi:10.1007/s00223-001-
583 2115-6.
- 584 Borrmann, H., and Berner, M. 1983. Zum saisonalen Längenwachstum des Arkonasee-Dorsches
585 nach Wiederfangdaten von Markierungsexperimenten. Fisch. Forsch. **23**: 1–5.
- 586 Campana, S.E. 1999. Chemistry and composition of fish otoliths: pathways, mechanisms and
587 applications. Mar. Ecol. Prog. Ser. **188**: 263–297. doi:10.3354/meps188263.
- 588 Campana, S.E. 2001. Accuracy, precision and quality control in age determination, including a
589 review of the use and abuse of age validation methods. J. Fish Biol. **59**: 197–242.
590 doi:10.1111/j.1095-8649.2001.tb00127.x.
- 591 Campana, S.E., Mohn, R.K., Smith, S.J., and Chouinard, G.A. 1995. Spatial implications of a
592 temperature based growth model for Atlantic cod (*Gadus morhua*) off the eastern coast of
593 Canada. Can. J. Fish. Aquat. Sci. **52**: 2445–2456.
- 594 Clarke, L.M., and Friedland, K.D. 2004. Influence of growth and temperature on strontium

- deposition in the otoliths of Atlantic salmon. *J. Fish Biol.* **65**(3): 744–759.
doi:10.1111/j.0022-1112.2004.00480.x.
- Conley, D.J., Carestensen, J., Aigars, J., Bonsdorff, E., Eremina, T., Haahti, B.-M., Humborg, C.,
Jonssibm P., Kotta, J., Lännegren, C., Larsson, U., Maximov, A., Rodrigues Medina, M.,
Lysiak-Pastuszak, E., Remeikaite-Nikiene, N., Walve, J., Wilhelms, S., and Zillén, L. 2001.
Hypoxia is increasing in the coastal zone of the Baltic Sea. *Env. Sci. Tech.* **45**: 6777-6783.
doi:10.1021/es201212r.
- Constantine, W. 2007. Local maxima [R package]. Available from:
<https://www.rdocumentation.org/packages/splus2R/versions/1.0-1/topics/peaks> [accessed 17
August 2020].
- DECODE. 2009. Improved mEthodology for Baltic COD Age Estimation [Report]. Available
from: http://ec.europa.eu/fisheries/documentation/studies/cod_age_en.pdf.
- Doubleday, Z.A., Harris, H.H., Izzo, C., and Gillanders, B.M. 2014. Strontium randomly
substituting for calcium in fish otolith aragonite. *Anal. Chem.* **86**(1): 865–869.
doi:10.1021/ac4034278.
- Doubleday, Z., Izzo, C., Woodcock, S., and Gillanders, B.M. 2013. Relative contribution of water
and diet to otolith chemistry in freshwater fish. *Aquat. Biol.* **18**(3), 271–280.
doi:10.3354/ab00511.
- Eero, M., Hjelm, J., Behrens, J., Buchmann, K., Cardinale, M., Casini, M., Gasyukov, P.,
Holmgren, N., Horbowy, J., Hüsey, K., Kirkegaard, E., Kornilovs, G., Krumme, U., Köster,
F.W., Oeberst, R., Plikshs, M., Radtke, K., Raid, T., Schmidt, J., Tomczak, M.T., Vinther,
M., Zimmermann, C., and Storr-Paulsen, M. 2015. Eastern Baltic cod in distress: Biological
changes and challenges for stock assessment. *ICES J. Mar. Sci.* **72**(8), 2180–2186.

- 618 doi:10.1093/icesjms/fsv109.
- 619 Friedrich, L.A., and Halden, N.M. 2010. Determining Exposure History of Northern Pike and
- 620 Walleye to Tailings Effluence Using Trace Metal Uptake in Otoliths. *Env. Sci. Tech.* **44**(5):
- 621 1551–1558. doi:10.1021/es903261q.
- 622 Funk, S., Krumme, U., Temming, A., and Möllmann, C. 2020. Gillnet fishers' knowledge reveals
- 623 seasonality in depth and habitat use of cod (*Gadus morhua*) in the Western Baltic Sea. *ICES*
- 624 *J. Mar. Sci.* doi:10.1093/icesjms/fsaa071.
- 625 Granzotto, A., Franceschini, G., Malavasi, S., Molin, G., Pranovi, F., and Torricelli, P. 2003.
- 626 Marginal increment analysis and Sr/Ca ratio in otoliths of the grass goby, *Zosterisessor*
- 627 *ophiocephalus*. *It. J. Zool.* **70**(1): 5–11. doi:10.1080/11250000309356489.
- 628 Halden, N.M., and Friedrich, L.A. 2008. Trace-element distributions in fish otoliths: natural
- 629 markers of life histories, environmental conditions and exposure to tailings effluence. *Min.*
- 630 *Mag.* **72**(2): 593–605. doi:10.1180/minmag.2008.072.2.593.
- 631 Halden, N.M., Mejia, S.R., Babaluk, J.A., Reist, J.D., Kristofferson, A.H., Campbell, J.L., and
- 632 Teesdale, W.J. 2000. Oscillatory zinc distribution in Arctic char (*Salvelinus alpinus*) otoliths:
- 633 The result of biology or environment? *Fish. Res.* **46**(1–3): 289–298. doi:10.1016/S0165-
- 634 7836(00)00154-5.
- 635 Heimbrand, Y., Limburg, K.E., Hüsey, K., Casini, M., Sjöberg, R., Palmén Bratt, A., Levinsky, S.-
- 636 E., Karpushevskaya, A., Radtke, K., and Öhlund, J. 2020. Seeking the True Time: Exploring
- 637 Otolith Chemistry as an Age-Determination Tool. *J. Fish Biol.* jfb.14422.
- 638 doi:10.1111/jfb.14422.
- 639 Hemmer-Hansen, J., Hüsey, K., Baktoft, H., Huwer, B., Bekkevold, D., Haslob, H., Herrmann, J.-
- 640 P., Hinrichsen, H.-H., Krumme, U., Mosegaard, H., Nielsen, E.E., Reusch, T.B. H, Storr-

- 641 Paulsen, M., Velasco, A., von Dewitz, B., Dierking, J., Eero, M. 2019. Genetic analyses
642 reveal complex dynamics within a marine fish management area. *Evol. Appl.* doi:12: 830–
643 844.
- 644 Høie, H., and Folkvord, A. 2006. Estimating the timing of growth rings in Atlantic cod otoliths
645 using stable oxygen isotopes. *J. Fish Biol.* **68**(3): 826–837. doi:10.1111/j.0022-
646 1112.2006.00957.x.
- 647 Hüsey, K., Nielsen, B., Mosegaard, H., and Clausen, L. 2009. Using data storage tags to link otolith
648 macro- structure in Baltic cod *Gadus morhua* with environmental conditions. *Mar. Ecol.*
649 *Prog. Ser.* **378**: 161–170. doi:10.3354/meps07876.
- 650 Hüsey, K. 2010. Why is age determination of Baltic cod (*Gadus morhua*) so difficult? *ICES J. Mar.*
651 *Sci.* **67**(6): 1198–1205. doi:10.1093/icesjms/fsq023.
- 652 Hüsey, K., Casini, M., Haase, S., Hilvarsson, A., Horbowy, J., Krüger-Johnsen, M., Krumme, U.,
653 Limburg, K. E., McQueen, K., Mion, M., Olesen, H. J., and Radtke, K. 2020b. Tagging Baltic
654 Cod – TABACOD. Eastern Baltic cod: Solving the ageing and stock assessment problems
655 with combined state-of-the-art tagging methods. DTU Aqua Report no. 368-2020. National
656 Institute of Aquatic Resources, Technical University of Denmark. 64 pp. ISBN:978-87-7481-
657 290-6.
- 658 Hüsey, K., Gröger, J., Heidemann, F., Hinrichsen, H.-H., and Marohn, L. 2016. Slave to the rhythm:
659 Seasonal signals in otolith microchemistry reveal age of eastern Baltic cod (*Gadus morhua*).
660 *ICES J. Mar. Sci.* **73**(4): 1019–1032. doi:10.1093/icesjms/fsv247.
- 661 Hüsey, K., Hinrichsen, H.-H., Fey, D.P., Walther, Y., and Velasco, A. 2010. The use of otolith
662 microstructure to estimate age in adult Atlantic cod *Gadus morhua*. *J. Fish Biol.* **76**(7), 1640–
663 1654. doi:10.1111/j.1095-8649.2010.02602.x.

- 664 Hüssy, K., St.John, M.A., and Böttcher, U. 1997. Food resource utilization by juvenile Baltic cod
665 *Gadus morhua*: A mechanism potentially influencing recruitment success at the demersal
666 juvenile stage? Mar. Ecol. Prog. Ser. **155**: 199–208. doi:10.3354/meps155199.
- 667 Hüssy, Karin, Eero, M., and Radtke, K. 2018. Faster or slower: has growth of eastern Baltic cod
668 changed? Mar. Biol. Res. **14**(6): 598–609. doi:10.1080/17451000.2018.1502446.
- 669 Hüssy, Karin, Limburg, K.E., de Pontual, H., Thomas, O.R.B., Cook, P.K., Heimbrand, Y., Blass,
670 M., and Sturrock, A.M. 2020. Trace Element Patterns in Otoliths: The Role of
671 Biomineralization. Rev. Fish. Sci. Aquacult. 1–33. doi:10.1080/23308249.2020.1760204.
- 672 Hüssy, Karin, Radtke, K., Plikshs, M., Oeberst, R., Baranova, T., Krumme, U., Sjöberg, R.,
673 Walther, Y., and Mosegaard, H. 2016. Challenging ICES age estimation protocols: lessons
674 learned from the eastern Baltic cod stock. ICES J. Mar. Sci. **73**(9): 2138–2149.
675 doi:10.1093/icesjms/fsw107.
- 676 ICES. 2014. Report of the Baltic Fisheries Assessment Working Group (WGBFAS). 3–10 April
677 2014 ICES HQ. Copenhagen, Denmark. ICES CM 2014/ ACOM:10.
- 678 ICES. 2015. Report of the Benchmark Workshop on Baltic Cod Stocks (WKBALTCOD). 2–6
679 March 2015, Rostock, Germany. ICES CM 2015/ACOM:35.
- 680 Izzo, C., Doubleday, Z.A., and Gillanders, B.M. 2016. Where do elements bind within the otoliths
681 of fish? Mar. Fresh. Res. **67**(7): 1072–1076. doi:10.1071/MF15064.
- 682 Jochum, K.P., Weis, U., Schwager, B., Stoll, B., Wilson, S.A., Haug, G.H., Andreae, M.O., and
683 Enzweiler, J. 2016. Reference Values Following ISO Guidelines for Frequently Requested
684 Rock Reference Materials. Geost. Geoanal. Res. **40**(3): 333-350. doi:10.1111/j.1751-
685 908X.2015.00392.x.
- 686 Jochum, K.P., Weis, U., Stoll, B., Kuzmin, D., Yang, Q., Raczek, I., Jacob, D.E., Stracke, A.,

- 687 Birbaum, K., Frick, D.A., Günther, D., and Enzweiler, J. 2011. Determination of Reference
688 Values for NIST SRM 610-617 Glasses Following ISO Guidelines. *Geost. Geoanal. Res.*
689 **35**(4): 397-429. doi:10.1111/j.1751-908X.2011.00120.x.
- 690 Kalish, J.M. 1991. Determinants of otolith chemistry: seasonal variation in the composition of
691 blood plasma, endolymph and otoliths of bearded rock cod *Pseudophycis barbatus*. *Mar.*
692 *Ecol. Prog. Ser.* **74**: 137–159. doi: 10.2307/24825820.
- 693 Kraus, R. T., and Secor, D. H. 2004. Incorporation of strontium into otoliths of an estuarine fish. *J.*
694 *Exp. Mar. Biol. Ecol.* **302**(1): 85–106. doi:10.1016/J.JEMBE.2003.10.004.
- 695 Limburg, K.E., Olson, C., Walther, Y., Dale, D., Slomo, C.P., and Høie, H. 2011. Tracking Baltic
696 hypoxia and cod migration over millennia with natural tags. *Proc. Nat. Acad. Sci. US* **108**(22),
697 E177–E182. doi:10.1073/pnas.1100684108
- 698 Limburg, K.E., and Casini, M. 2018. Effect of Marine Hypoxia on Baltic Sea Cod *Gadus morhua*:
699 Evidence From Otolith Chemical Proxies. *Front. Mar. Sci.* **5**: 482.
700 doi:10.3389/fmars.2018.00482.
- 701 Limburg, K.E., and Elfman, M. 2010. Patterns and magnitude of Zn:Ca in otoliths support the recent
702 phylogenetic typology of Salmoniformes and their sister groups. *Can. J. Fish. Aquat. Sci.*
703 **67**(4): 597–604. doi:10.1139/f10-014.
- 704 Limburg, K.E., Wuenschel, M.J., Hüsey, K., Heimbrand, Y., and Samson, M. 2018. Making the
705 Otolith Magnesium Chemical Calendar-Clock Tick: Plausible Mechanism and Empirical
706 Evidence. *Rev. Fish. Sci. Aquacult.* **26**(4), 479–493. doi:10.1080/23308249.2018.1458817
- 707 MARNET. 2020. Data of the automated measuring stations (MARNET) [Data repository].
708 Available from: <https://www.io-warnemuende.de/marnet-arkona-sea.html> [accessed 19 April
709 2020].

- 710 McQueen, K., Casini, M., Dolk, B., Haase, S., Hemmer-Hansen, J., Hilvarsson, A., Hüsey, K.,
711 Mion, M., Mohr, T., Radtke, K., Schade, F.M., Schulz, N., and Krumme, U. 2020. Regional
712 and stock-specific differences in contemporary growth of Baltic cod revealed through tag-
713 recapture data. ICES J. Mar. Sci. doi:10.1093/icesjms/fsaa104.
- 714 McQueen, K., Eveson, J.P., Dolk, B., Lorenz, T., Mohr, T., Schade, F.M., and Krumme, U. 2019.
715 Growth of cod (*Gadus morhua*) in the western Baltic Sea: estimating improved growth
716 parameters from tag–recapture data. Can. J. Fish. Aquat. Sci. **76**(8): 1326–1337.
717 doi:10.1139/cjfas-2018-0081.
- 718 Mello, L.G.S., and Rose, G.A. 2005. Seasonal growth of Atlantic cod: effects of temperature,
719 feeding and reproduction. J. Fish Biol. **67**(1): 149–170. doi:10.1111/j.0022-
720 1112.2005.00721.x.
- 721 Miller, M.B., Clough, A.M., Batson, J.N., and Vachet, R.W. 2006. Transition metal binding to cod
722 otolith proteins. J. Exp. Mar. Biol. Ecol. **329**(1): 135–143.
723 doi:10.1016/J.JEMBE.2005.08.016.
- 724 Mion, M., Haase, S., Hemmer-Hansen, J., Hilvarsson, A., Hüsey, K., Krüger-Johnsen, M., Krumme,
725 U., McQueen, K., Plikshs, M., Radtke, K., Schade, F.M., Vitale, F., Casini, M. Multidecadal
726 changes in fish growth rates estimated from tagging data: a case study from the Eastern Baltic
727 cod stock. Fish Fish. (in review, Manuscript ID FaF-20-Jun-OA-158).
- 728 Mion, M., Hilvarsson, A., Hüsey, K., Krumme, U., Krüger-Johnsen, M., McQueen, K., Mohamed,
729 E., Motyka, R., Orio, A., Plikshs, M., Radtke, K., and Casini, M. 2020. Historical growth of
730 Eastern Baltic cod (*Gadus morhua*): Setting a baseline with international tagging data. Fish.
731 Res. **223**: 105442. doi:10.1016/j.fishres.2019.105442.
- 732 Mohan, J., and Walther, B. 2016. Out of breath and hungry: natural tags reveal trophic resilience

- 733 of Atlantic croaker to hypoxia exposure. Mar. Ecol. Prog. Ser. **560**: 207–221.
 734 doi:10.3354/meps11934.
- 735 Morita, K., Morita, S. H., Nagasawa, T., and Kuroki, M. 2013. Migratory patterns of anadromous
 736 white-spotted charr *Salvelinus leucomaenis* in Eastern Hokkaido, Japan: The solution to a
 737 mystery? J. Ichthyol. **53**(10): 809–819. doi:10.1134/S0032945213100068.
- 738 Nielsen, B., Hüsey, K., Neuenfeldt, S., Tomkiewicz, J., Behrens, J.W., and Andersen, K.H. 2013.
 739 Individual behaviour of Baltic cod *Gadus morhua* in relation to sex and reproductive state.
 740 Aquat. Biol. **18**(2): 197–207. doi:10.3354/ab00505.
- 741 Oeberst, R. 2008. Distribution pattern of cod and flounder in the Baltic Sea based on international
 742 coordinated trawl surveys. ICES CM, 2008/J:09(28).
- 743 Payan, P., de Pontual, H., Bœuf, G., and Mayer-Gostan, N. 2004. Endolymph chemistry and otolith
 744 growth in fish. Com. Rend. Pale. **3**(6–7): 535–547. doi:10.1016/J.CRPV.2004.07.013.
- 745 Pihl, L. and Ulmestrand, M. 1993. Migration patterns of juvenile cod (*Gadus morhua*) on the
 746 Swedish west coast. ICES J. Mar. Sci. **50**(1): 63-70.
- 747 Pihl, L. 1982. Food intake of young cod and flounder in a shallow bay on the Swedish west coast.
 748 Neth. J. Sea Res. **15**(3), 419-432.
- 749 Pörtner, H. O., Berdal, B., Blust, R., Brix, O., Colosimo, A., De Wachter, B., Giuliani, A., Johansen,
 750 T., Fischer, T., Knust, R., Lannig, G., Naevdal, G., Nedenes, A., Nyhammer, G., Sartoris, F.
 751 J., Serendero, I., Sirabella, P., Thorkildsen, S. and Zakhartsev, M. 2001. Climate induced
 752 temperature effects on growth performance, fecundity and recruitment in marine fish:
 753 Developing a hypothesis for cause and effect relationships in Atlantic cod (*Gadus morhua*)
 754 and common eelpout (*Zoarces viviparus*). Cont. Shelf Res. **21**(18–19): 1975–1997.
 755 doi:10.1016/S0278-4343(01)00038-3.

- 756 R Development Core Team. 2020. R: A Language and Environment for Statistical Computing.
757 [Software] R Foundation for Statistical Computing. R Foundation for Statistical Computing,
758 Vienna, Austria. Available from: <http://www.r-project.org> [accessed 5 October 2020].
- 759 Ranaldi, M.M., and Gagnon, M.M. 2008. Trace Metal Incorporation in Otoliths of Black Bream
760 (*Acanthopagrus butcheri* Munro), an Indicator of Exposure to Metal Contamination. Water
761 Air Soil Pol. **194**(1–4): 31–43. doi:10.1007/s11270-008-9696-x.
- 762 Righton, D.A., Andersen, K.H., Neat, F., Thorsteinsson, V., Steingrund, P., Svedäng, H.,
763 Michalsen, K., Hinrichsen, H.-H., Bendall, V., Neuenfeldt, S., Wright, P.J., Jonsson, P., Huse,
764 G., Van Der Kooij, J., Mosegaard, H., Hüsey, K., and Metcalfe, J. 2010. Thermal niche of
765 Atlantic cod *Gadus morhua*: Limits, tolerance and optima. Mar. Ecol. Prog. Ser. **420**: 1–13.
766 doi:10.3354/meps08889.
- 767 Rolff, C., Elmgren, R., and Voss, M. 2008. Deposition of nitrogen and phosphorus on the Baltic
768 Sea: seasonal patterns and nitrogen isotope composition. Biogeosci. Disc. **5**:1657-1667. doi:
769 biogeosciences-discuss.net/5/3013/2008.
- 770 Schade, F., Weist, P., and Krumme, U. 2019. Evaluation of four stock discrimination methods to
771 assign individuals from mixed-stock fisheries using genetically validated baseline samples.
772 Mar. Ecol. Prog. Ser. **627**: 125–139. doi: 10.3354/meps13061.
- 773 Schwalme, K., and Chouinard, G.A. 1999. Seasonal dynamics in feeding, organ weights, and
774 reproductive maturation of Atlantic cod (*Gadus morhua*) in the southern Gulf of St.
775 Lawrence. ICES J. Mar. Sci. **56**: 303–319. doi: 10.1006/jmsc.1999.0458.
- 776 Serre, S.H., Hüsey, K., Nielsen, K.E., Fink-Jensen, P., and Thomsen, T.B. 2018. Analysis of cod
777 otolith microchemistry by continuous line transects using LA-ICP-MS. Geol. Surv. Den.
778 Greenl. Bull. **41**: 91–94. doi:1604-8156.

- 779 Seyama, H., Edmonds, J.S., Moran, M.J., Shibata, Y., Soma, M., and Morita, M. 1991. Periodicity
780 in fish otolith Sr, Na, and K corresponds with visual banding. *Expri.* **47**: 1193–1196.
- 781 Shearer, K.D., and Åsgård, T. 1992. The effect of water-borne magnesium on the dietary
782 magnesium requirement of the rainbow trout (*Oncorhynchus mykiss*). *Fish Physiol. Biochem.*
783 **9**(5–6): 387–392. doi:10.1007/BF02274219.
- 784 Siskey, M.R., Lyubchich, V., Liang, D., Piccoli, P.M., and Secor, D.H. 2016. Periodicity of
785 strontium: Calcium across annuli further validates otolith-ageing for Atlantic bluefin tuna
786 (*Thunnus thynnus*). *Fish. Res.* **177**: 13–17. doi:10.1016/j.fishres.2016.01.004.
- 787 Sturrock, A.M., Hunter, E., Milton, J.A., Johnson, R.C., Waring, C.P., and Trueman, C.N. 2015.
788 Quantifying physiological influences on otolith microchemistry. *Met. Ecol. Evol.* **6**(7): 806–
789 816. doi:10.1111/2041-210X.12381.
- 790 Sturrock, A.M., Trueman, C.N., Darnaude, A.M., and Hunter, E. 2012. Can otolith elemental
791 chemistry retrospectively track migrations in fully marine fishes? *J. Fish Biol.* **81**(2): 766–
792 795. doi:10.1111/j.1095-8649.2012.03372.x.
- 793 Swaileh, K.M., and Adelung, D. 1995. Effect of body size and season on the concentrations of Cu,
794 Cd, Pb and Zn in *Diastylis rathkei* (kröyer) (Crustacea: Cumacea) from Kiel Bay, Western
795 Baltic. *Mar. Poll. Bul.* **31**(1–3): 103–107. doi:10.1016/0025-326X(94)00258-B.
- 796 Thomas, O.R.B., and Swearer, S.E. 2019. Otolith Biochemistry—A Review. *Rev. Fish. Sci. Aquac.*
797 **27**(4): 458–489. doi:10.1080/23308249.2019.1627285.
- 798 Thomas, O.R.B., Ganio, K., Roberts, B.R., and Swearer, S.E. 2017. Trace element–protein
799 interactions in endolymph from the inner ear of fish: implications for environmental
800 reconstructions using fish otolith chemistry. *Metall.* **9**(3): 239–249.
801 doi:10.1039/C6MT00189K.

- 802 Tomás, J., Geffen, A.J., Millner, R.S., Piñeiro, C.G and Tserpes, G. 2006. Elemental composition
803 of otolith growth marks in three geographically separated populations of European hake
804 (*Merluccius merluccius*). Mar. Biol. **148**: 1399-1413. doi: 10.1007/s00227-005-0171-6.
- 805 Viktorsson L. 2017. Hydrography and oxygen in the deep basins. HELCOM Baltic Sea
806 Environment Fact Sheets (BSEFS). pp 7 [Report] Available from: [https://helcom.fi/wp-](https://helcom.fi/wp-content/uploads/2020/07/BSEFS-Sea-Surface-Temperature-in-the-Baltic-Sea-2018.pdf)
807 [content/uploads/2020/07/BSEFS-Sea-Surface-Temperature-in-the-Baltic-Sea-2018.pdf](https://helcom.fi/wp-content/uploads/2020/07/BSEFS-Sea-Surface-Temperature-in-the-Baltic-Sea-2018.pdf)
808 [accessed 25 August 2020].
- 809 Viktorsson, L., Ekeröth, N., Nilsson, M., Kononets, M., and Hall, P.O.J. 2013. Phosphorus
810 recycling in sediments of the central Baltic Sea. Biogeosci. **10**: 3901-3916. doi:10.5194/bg-
811 10-3901-2013.
- 812 Walther, B.D., and Thorrold, S.R. 2006. Water, not food, contributes the majority of strontium and
813 barium deposited in the otoliths of a marine fish. Mar. Ecol. Prog. Ser. **311**: 125–130.
814 doi:10.3354/meps311125.
- 815 Weidman, C.R., and Millner, R. 2000. High-resolution stable isotope records from North Atlantic
816 cod. Fish. Res. **46**(1–3): 327–342. doi:10.1016/S0165-7836(00)00157-0.
- 817 Wenne, R., Bернаś, R., Kijewska, A., Pócwierz-Kotus, A., Strand, J., Petereit, C., Plaуска, K., Sics,
818 I., Árnýasi, M., and Kent, M.P. 2020. SNP genotyping reveals substructuring in weakly
819 differentiated populations of Atlantic cod (*Gadus morhua*) from diverse environments in the
820 Baltic Sea. Sci. Rep. **10**: 9738. doi: s41598-020-66518-4.
- 821 Wieland, K., Jarre-Teichmann, A., and Horbowa, K. 2000. Changes in the timing of spawning of
822 Baltic cod: possible causes and implications for recruitment. ICES J. Mar. Sci. **57**(2): 452–
823 464. doi:1006/jmsc.1999.0522.
- 824 Wulff, F., and Rahm, L. 1988. Long-term, seasonal and spatial variations of nitrogen, phosphorus

825 and silicate in the Baltic; An overview. *Mer. Env. Res.* **26**(1):19-37. doi:10.1016/0141-
826 1136(88)90032-3.

827

Figure captions

Fig. 1. Map of the locations of cod from three different samples used in this study. Green symbols: Known-age samples of Baltic cod from the “Improved methodology for Baltic COD Age Estimation” (DECODE) project where age was obtained from patterns in daily otolith increment widths (varying size indicative of sample size). Blue and red symbols: Samples of recaptured Baltic cod from the international tagging project “Tagging Baltic Cod” (TABACOD), where symbols show the recapture locations of tagged cod (eastern Baltic cod = blue symbols; western Baltic cod = red symbols). Black symbols: Samples of cod from the Kattegat, which have a high contrast between otolith growth zones and therefore are used as test group to identify the best approach for the analyses of element profiles. Numbers identify ICES Subdivisions (SD), where SD 21: Kattegat, SD 22: Belt Sea, SD 23: Sound, SD 24: Arkona Sea, SD 25 Bornholm Sea, SD 26: Gdansk Bay and SD 28: Gotland Basin. The area consists of three management areas: Kattegat (SD 21), western Baltic Sea (SD 22 – 24) and eastern Baltic Sea (SD 25 – 32). Map created using the “maps” package ver. 3.3.0 of “R”.

Fig. 2. Transversal section of an otolith from a 4-year old cod caught in December 2010 in Kattegat from the test sample (*TEST*) characterized by high contrast between seasonal translucent and opaque zones with concurrent high age estimation precision and well established ageing protocols. *TEST* samples were used to identify the best setting for profile smoothing and peak detection. Otolith section is viewed under reflected light, with superimposed elemental profile of phosphorus (as P/Ca ratio) from the nucleus to the dorsal otolith edge and translucent seasonal growth zones indicated by grey vertical bars.

Fig. 3. Transversal section of otolith of a 3-year old Baltic cod from the first validation collection, the *DECODE* samples, where age was obtained from patterns in daily otolith increment widths, viewed under reflected light (bottom right), where the black box indicates the otolith area viewed under 20x magnification and transmitted light (middle image). In this image, white dots indicate daily increments prior to and after a zone with no visible increments. The profile of daily increment widths from core to otolith edge (top left) shows how “winter zones” were identified. Winter zones (*WZ*) are indicated with arrows, where the distance of the midpoint of each zone to the core is the measurement used in the present analyses. Note that the last *WZ* has just started to form at the edge of the otolith and can therefore not be measured. Since the cod was caught in February and new growth zones are counted from the 1st January, this last zone corresponding to the edge, is counted when estimating the age of the fish. The arrows in the images of otolith cross section and magnified otolith zone showing daily increments correspond to the *WZ* identified in daily increment profile (top left).

Fig. 4. Transversal section of a tagged eastern Baltic cod otolith from the second validation sample, the *TABACOD* samples consisting of tagged and recaptured cod from the from the international tagging project “Tagging Baltic Cod”, viewed under reflected light with the position of the laser transect indicated with a broken black line. The same otolith is shown under UV light showing the green fluorescent TET mark induced at release, where the part of the profile used in this study is indicated with a solid black line on both images. The cod was released at 54.60 N and 13.42 E on the 03/11/2017 at a length of 263 mm and recaptured at a length of 462 mm at 54.69N and 13.19E on the 19/06/2019 after 593 days at liberty.

Fig. 5. Element profiles of a 4-year old, 290 mm long, male Baltic cod from the first validation collection, the *DECODE* samples, where age was obtained from patterns in daily otolith increment widths, including an image of the corresponding otolith viewed under reflected light. Profiles show relative element concentrations (Element:Ca ratios divided by the profile mean for each element) where data are loess smoothed means and confidence interval bands in relation to distance to the core along the dorsal growth axis. Grey vertical bars indicate the location of three consecutive winter zones (*WZ*) identified using daily increment patterns. Element minima (*Min*) = blue symbols, vertical lines from *Min* to x-axis are shown to facilitate the identification of the timing in relation to *WZ*. Incorporation mechanisms of the elements, i.e. whether element incorporation is expected to depend on environmental concentration, physiology or a combination of both, is indicated above each column. Note that the y-axis was truncated to optimize the visual appearance of the signals, and that this has excluded some of the highest concentrations in Cu, Mn, Zn and Pb at the beginning of the profiles.

Fig. 6. Relationship between minima in the chemical profiles (*Min*) for all elements separately in relation to winter zones (*WZ*) identified in the daily increment patterns of Baltic cod from the first validation collection, the *DECODE* samples, where age was obtained from patterns in daily otolith increment widths. Colours indicate consecutive number of *Min* and corresponding *WZ* identified. Black represents the first element *Min* and *WZ*, red and green represent the subsequent second and third *Min* and *WZ*. Incorporation mechanisms of the elements, i.e. whether element incorporation is expected to depend on environmental concentration, physiology or a combination of both, is indicated above each column..

Fig. 7. Frequency distributions of the difference between known age identified from daily increment patterns and chemical age from the number of profile minima ($WZ - Min$) by element in Baltic cod from the first validation collection, the *DECODE* samples, where age was obtained from patterns in daily otolith increment widths. Incorporation mechanisms of the elements, i.e. whether element incorporation is expected to depend on environmental concentration, physiology or a combination of both, is indicated above each column..

Fig. 8. Element profiles of a tagged and recaptured female eastern Baltic cod from the *TABACOD* validation samples from the international tagging project “Tagging Baltic Cod” with 927 days at liberty, including an image of the corresponding otolith view under reflected light (black bar indicates tagging period). Released on 14/11/2016, 54.574N, 13.825E at a length of 370mm; Recaptured on 30/05/2019, 55.377N, 15.647E at a length of 471 mm. Profiles show relative element concentrations (Element:Ca ratios divided by the profile mean for each element), from the TET mark to the otolith edge. Data are shown with loess smoothed means and confidence interval bands in relation to distance to the core. Element minima (Min) = blue symbols, element maxima (Max) = red symbols, vertical lines from Min to x-axis are shown to facilitate the identification of the time of the year corresponding to the extrema. Incorporation mechanisms of the elements is indicated above each column. Min in P occur in April in the years 2018 and 2019 and apparently somewhat earlier in 2017, albeit this minimum is difficult to estimate precisely owing to the limited data points between profile start and Min_{2017} . Min in Mg follow the same pattern but with a delay of approximately 1 month. Incorporation mechanisms of the elements, i.e. whether element

incorporation is expected to depend on environmental concentration, physiology or a combination of both, is indicated above each column.

Fig. 9. Elements where incorporation depends entirely on environmental concentration. Profiles are from the second validation samples, the *TABACOD* samples of tagged and recaptured Baltic cod with more than 180 days at liberty, from the TET mark to the otolith edge, in relation to date of incorporation. Left panel = eastern Baltic cod, right panes = western Baltic cod. Data shown are relative element concentrations (Element:Ca ratios divided by the profile mean for each element) with loess smoothed means and confidence interval bands. Minima (*Min*) = blue symbols, maxima (*Max*) = red symbols. Vertical lines from extrema to x-axis are shown to facilitate identification the time of the year corresponding to the extrema.

Fig. 10. Elements where incorporation is regulated by an interaction of environmental concentration and physiological processes. Profiles are from the second validation samples, the *TABACOD* samples of tagged and recaptured Baltic cod with more than 180 days at liberty, from the TET mark to the otolith edge, in relation to date of incorporation. Left panel = eastern Baltic cod, right panes = western Baltic cod. Data shown are relative element concentrations (Element:Ca ratios divided by the profile mean for each element) with loess smoothed means and confidence interval bands. Minima (*Min*) = blue symbols, maxima (*Max*) = red symbols. Vertical lines from extrema to x-axis are shown to facilitate identification the time of the year corresponding to the extrema.

941 **Fig. 11.** Elements where incorporation is regulated entirely by physiological processes. Profiles
942 are from the second validation samples, the *TABACOD* samples of tagged and recaptured Baltic
943 cod with more than 180 days at liberty, from the TET mark to the otolith edge, in relation to date
944 of incorporation. Left panel = eastern Baltic cod, right panes = western Baltic cod. Data shown are
945 relative element concentrations (Element:Ca ratios divided by the profile mean for each element)
946 with loess smoothed means and confidence interval bands. Minima (*Min*) = blue symbols, maxima
947 (*Max*) = red symbols. Vertical lines from extrema to x-axis are shown to facilitate identification
948 the time of the year corresponding to the extrema.

Can. J. Fish. Aquat. Sci. Downloaded from cdnsiencepub.com by Danmarks Tekniske Informationscenter - Danish Technical University (DTU) on 12/21/20
For personal use only. This Just-IN manuscript is the accepted manuscript prior to copy editing and page composition. It may differ from the final official version of record.

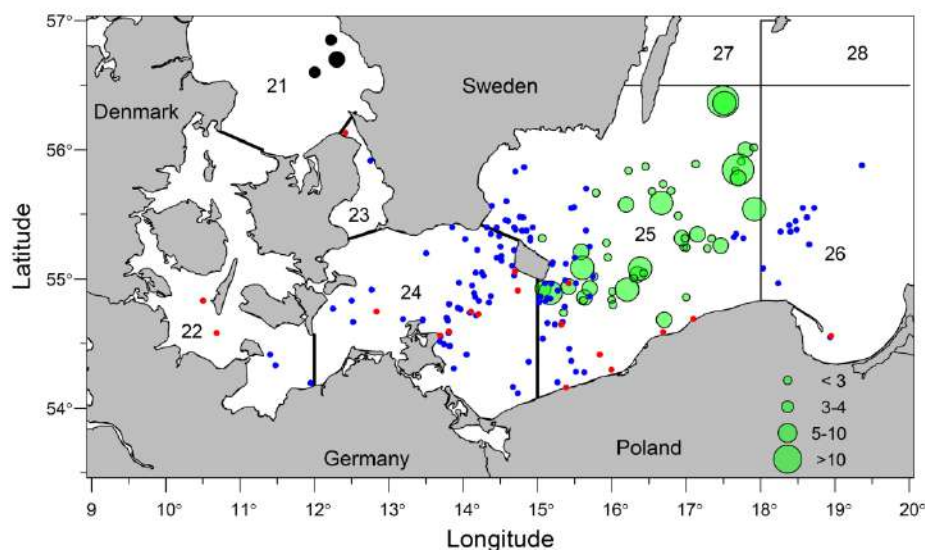
Table 1. Overview of samples used in this study. Values of length, age and days at liberty (DAL) are given as mean ± standard deviation with the range of values in brackets.

Collection	Stock	n	Length (mm)	Age (years)	DAL (days)
<i>TEST</i>	Kattegat	40	631±85 (390-830)	4.2 ± 0.5 (3 - 5)	na
<i>DECODE</i>	Eastern Baltic	53	242±64 (150-350)	3.2 ± 0.6 (2 - 4)	na
<i>TABACOD</i>	Eastern Baltic	123	438±53 (282–579) [†]	na	368±154 (183–927)
<i>TABACOD</i>	Western Baltic	20	467±76 (339–614) [†]	na	316±13 (186–748)

Footnote: [†] Length at recapture

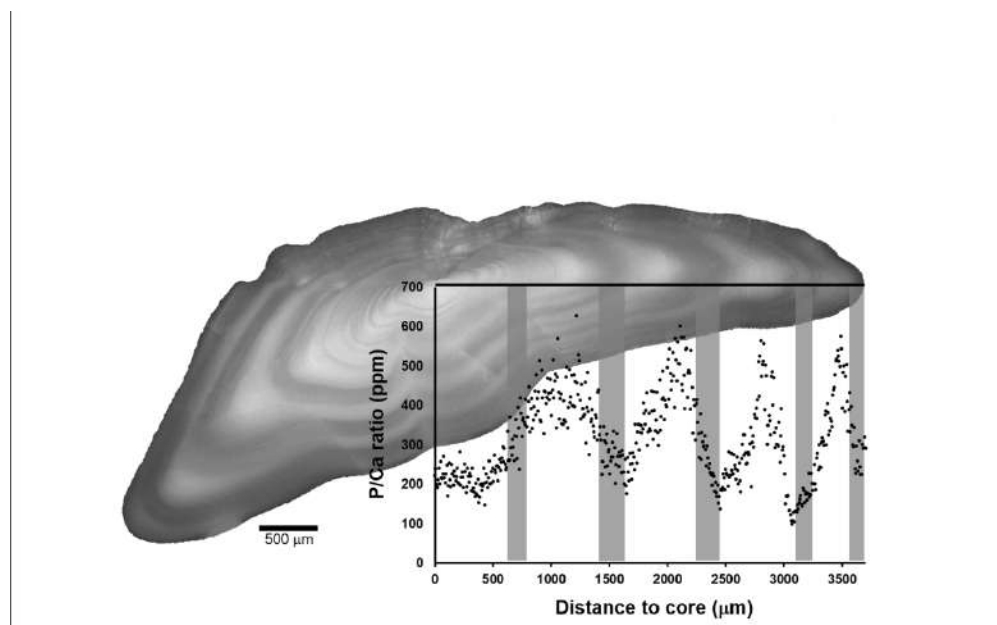
Table 2. Regression statistics of minima in the chemical profiles (*Min*) in relation to winter zones (*WZ*) in *DECODE* otoliths, confidence intervals in brackets.

Regulation	Element	Intercept	Slope	obs/groups	r ²
Environment	Ba	291 (190 – 392)	0.71 (0.64 – 0.79)	103/53	0.60
	Pb	104 (9 – 198)	0.82 (0.75 – 0.82)	114/53	0.73
	Sr	206 (87 – 325)	0.85 (0.76 – 0.93)	99/51	0.57
Physiology	Cu	150 (63 – 237)	0.79 (0.72 – 0.86)	105/52	0.67
	P	110 (26 – 193)	0.84 (0.77 – 0.91)	103/53	0.81
	Zn	166 (79 – 253)	0.81 (0.74 – 0.89)	110/53	0.73
Physiology and	Mg	177 (88 – 267)	0.88 (0.80 – 0.96)	102/53	0.73
Environment	Mn	305 (183 – 428)	0.76 (0.65 – 0.86)	90/51	0.62



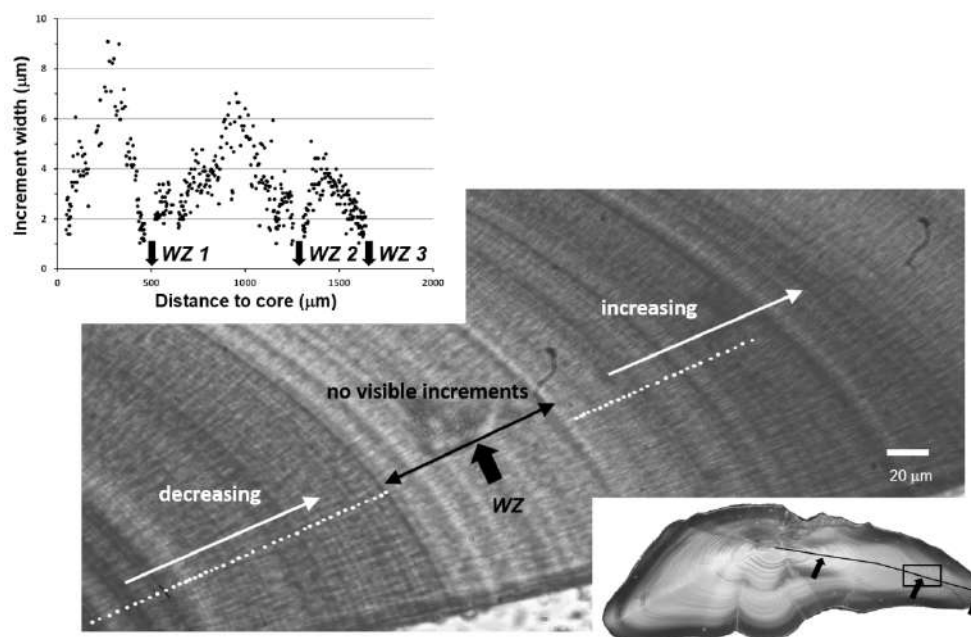
Map of the locations of cod from three different samples used in this study. Green symbols: Known-age samples of Baltic cod from the "Improved methodology for Baltic COD Age Estimation" (DECODE) project where age was obtained from patterns in daily otolith increment widths (varying size indicative of sample size). Blue and red symbols: Samples of recaptured Baltic cod from the international tagging project "Tagging Baltic Cod" (TABACOD), where symbols show the recapture locations of tagged cod (eastern Baltic cod = blue symbols; western Baltic cod = red symbols). Black symbols: Samples of cod from the Kattegat, which have a high contrast between otolith growth zones and therefore are used as test group to identify the best approach for the analyses of element profiles. Numbers identify ICES Subdivisions (SD), where SD 21: Kattegat, SD 22: Belt Sea, SD 23: Sound, SD 24: Arkona Sea, SD 25 Bornholm Sea, SD 26: Gdansk Bay and SD 28: Gotland Basin. The area consists of three management areas: Kattegat (SD 21), western Baltic Sea (SD 22 – 24) and eastern Baltic Sea (SD 25 – 32). Map created using the "maps" package ver. 3.3.0 of "R".

241x170mm (300 x 300 DPI)



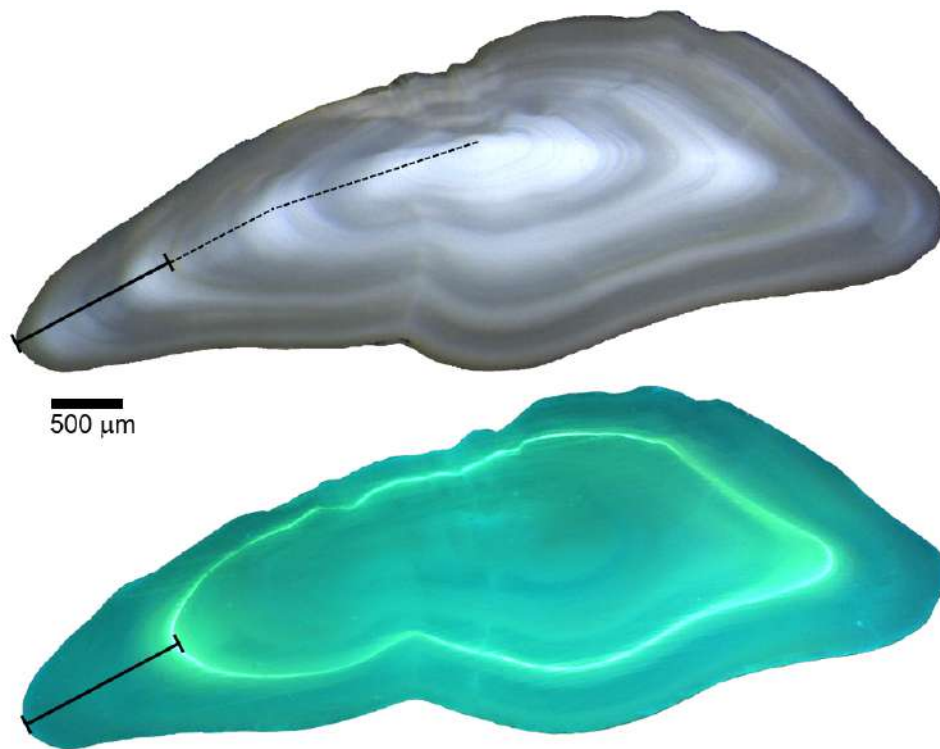
Transversal section of an otolith from a 4-year old cod caught in December 2010 in Kattegat from the test sample (TEST) characterized by high contrast between seasonal translucent and opaque zones with concurrent high age estimation precision and well established ageing protocols. TEST samples were used to identify the best setting for profile smoothing and peak detection. Otolith section is viewed under reflected light, with superimposed elemental profile of phosphorus (as P/Ca ratio) from the nucleus to the dorsal otolith edge and translucent seasonal growth zones indicated by grey vertical bars.

290x179mm (150 x 150 DPI)



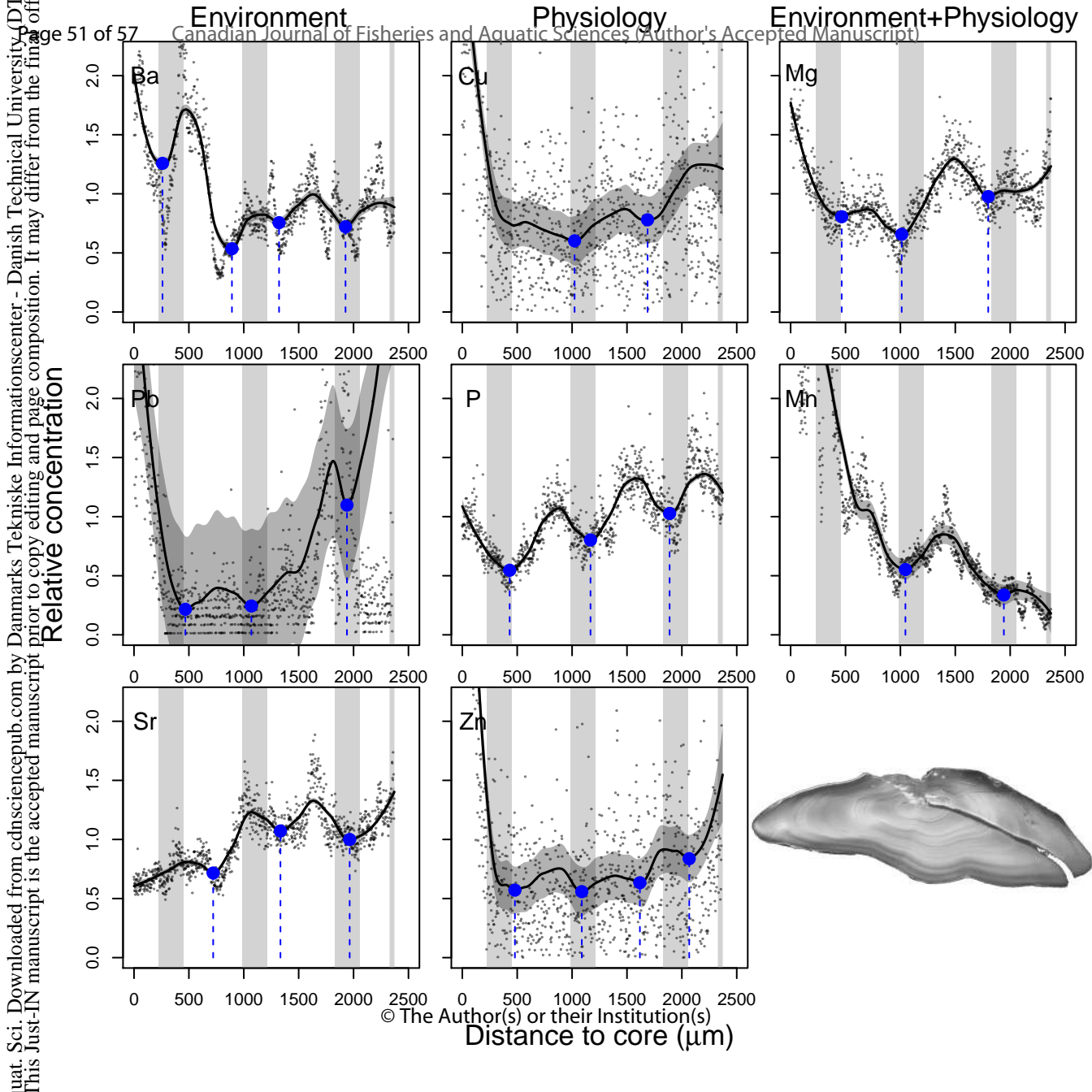
Transversal section of otolith of a 3-year old Baltic cod from the first validation collection, the DECODE samples, where age was obtained from patterns in daily otolith increment widths, viewed under reflected light (bottom right), where the black box indicates the otolith area viewed under 20x magnification and transmitted light (middle image). In this image, white dots indicate daily increments prior to and after a zone with no visible increments. The profile of daily increment widths from core to otolith edge (top left) shows how "winter zones" were identified. Winter zones (WZ) are indicated with arrows, where the distance of the midpoint of each zone to the core is the measurement used in the present analyses. Note that the last WZ has just started to form at the edge of the otolith and can therefore not be measured. Since the cod was caught in February and new growth zones are counted from the 1st January, this last zone corresponding to the edge, is counted when estimating the age of the fish. The arrows in the images of otolith cross section and magnified otolith zone showing daily increments correspond to the WZ identified in daily increment profile (top left).

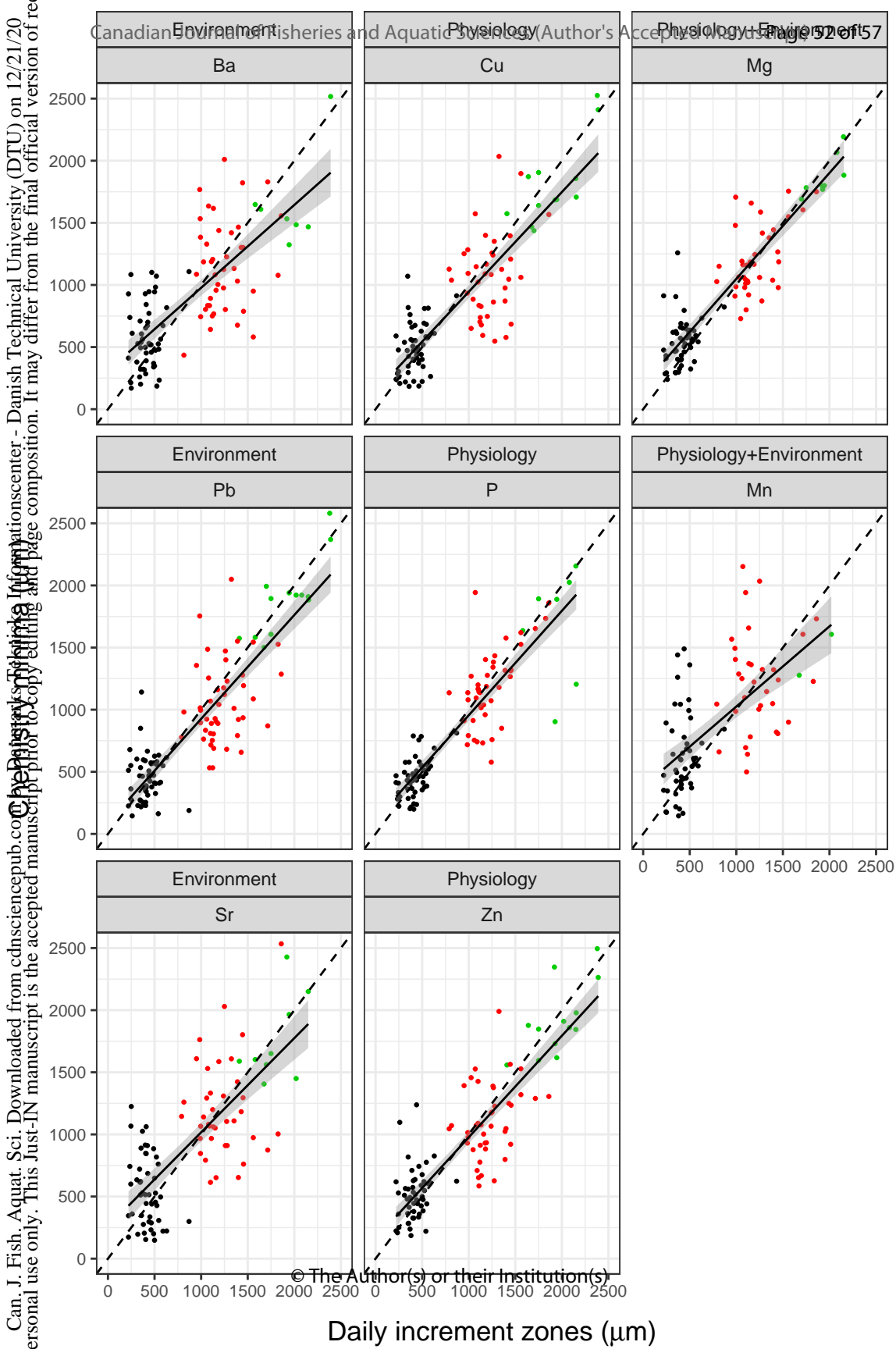
276x180mm (150 x 150 DPI)

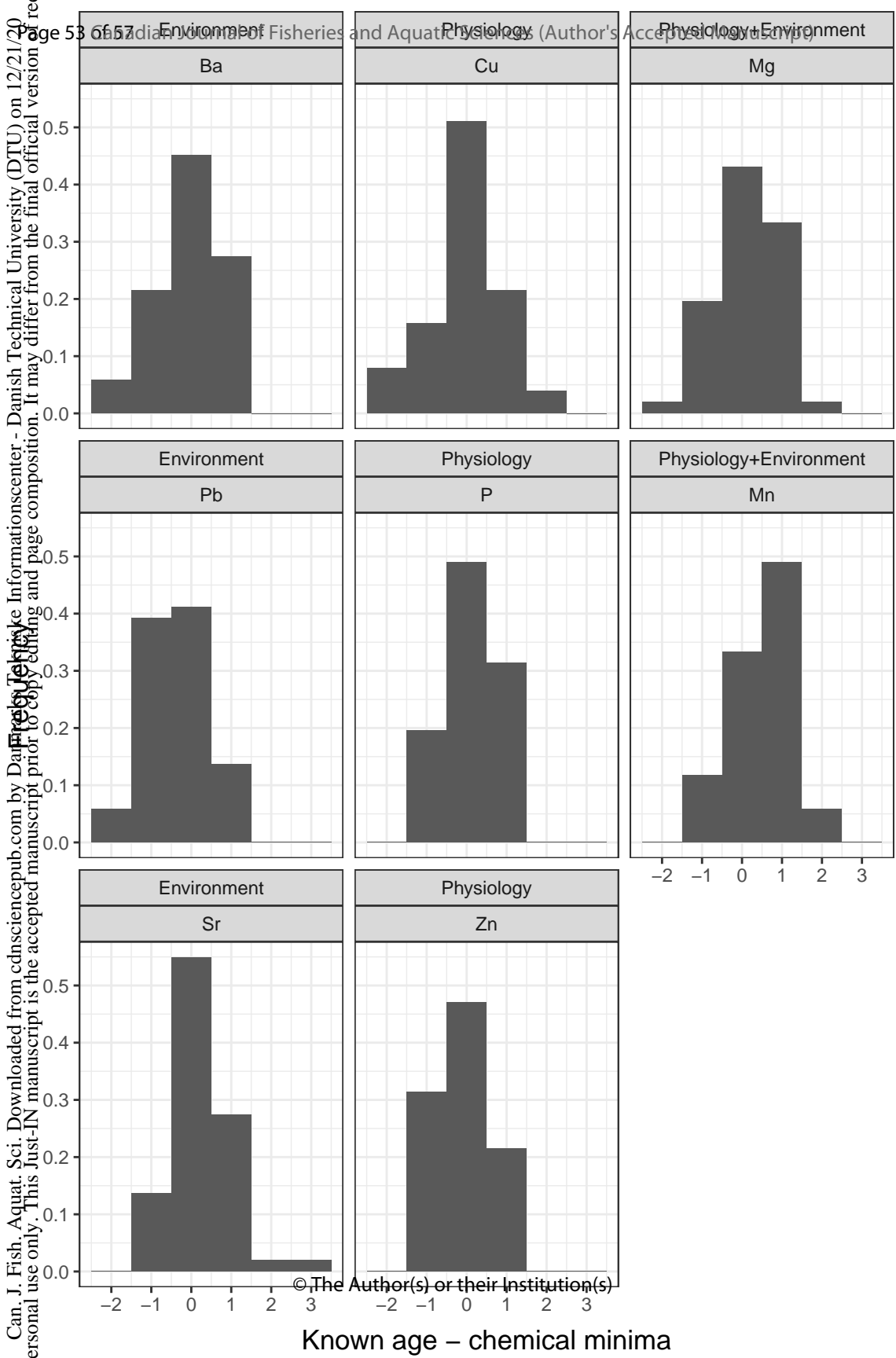


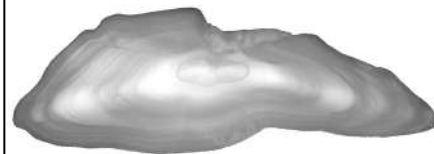
Transversal section of a tagged eastern Baltic cod otolith from the second validation sample, the TABACOD samples consisting of tagged and recaptured cod from the international tagging project "Tagging Baltic Cod", viewed under reflected light with the position of the laser transect indicated with a broken black line. The same otolith is shown under UV light showing the green fluorescent TET mark induced at release, where the part of the profile used in this study is indicated with a solid black line on both images. The cod was released at 54.60 N and 13.42 E on the 03/11/2017 at a length of 263 mm and recaptured at a length of 462 mm at 54.69N and 13.19E on the 19/06/2019 after 593 days at liberty.

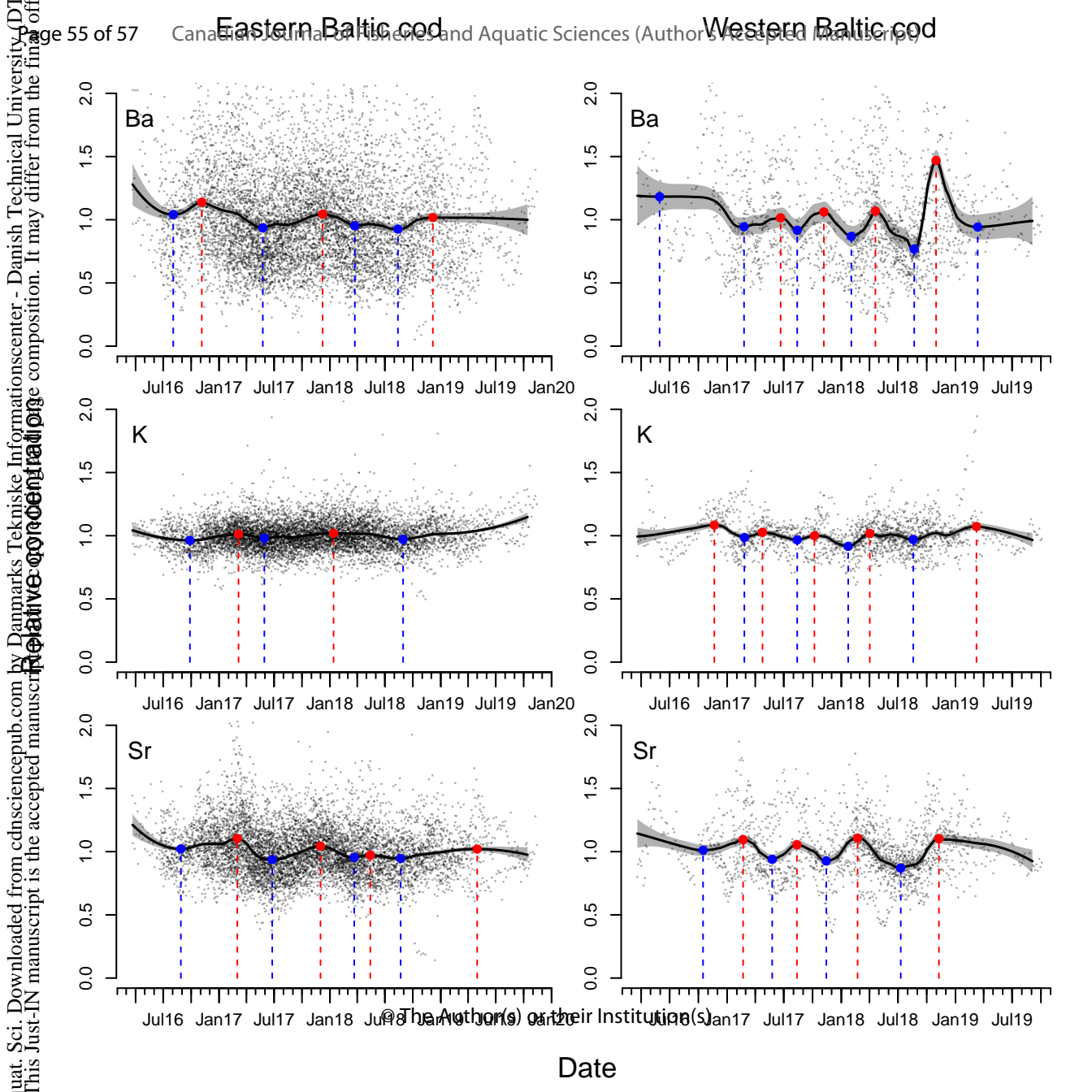
164x125mm (150 x 150 DPI)

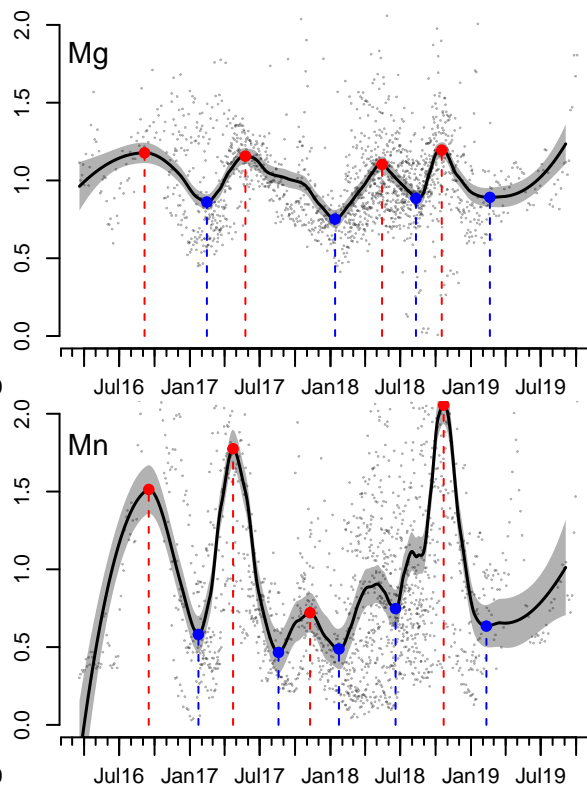
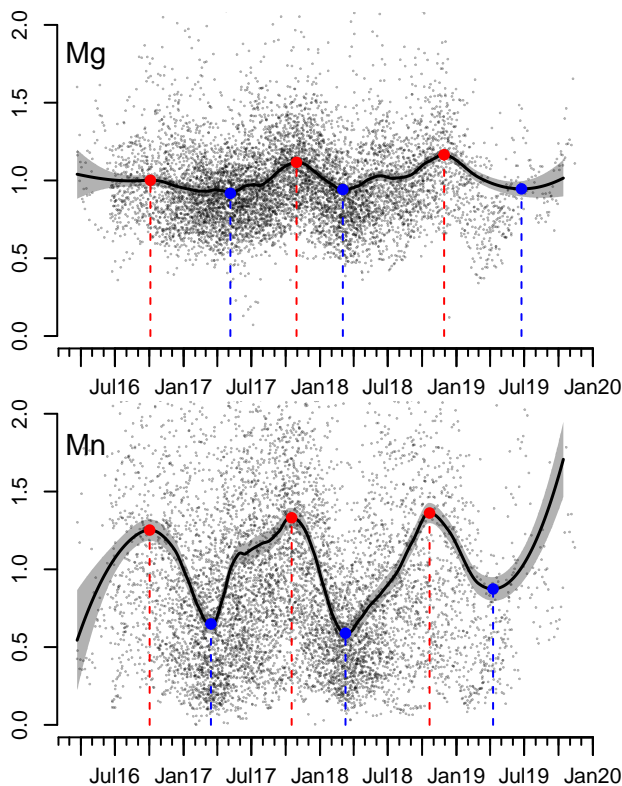




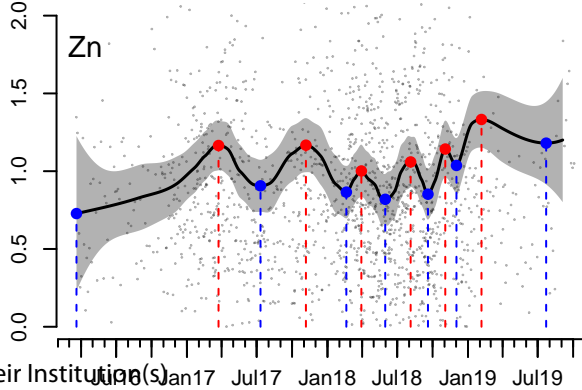
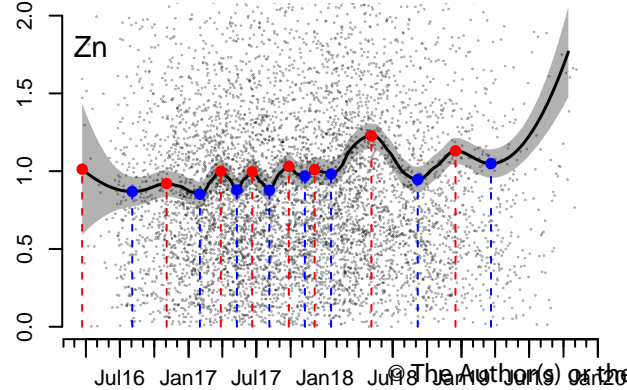
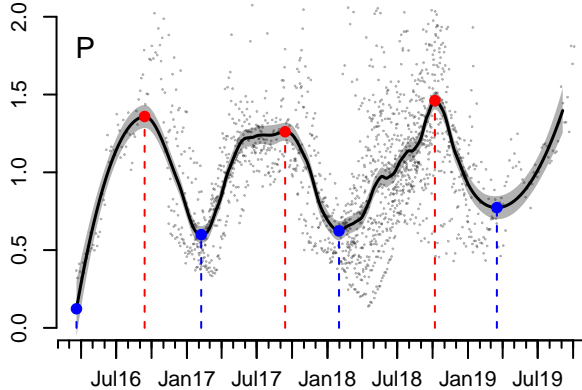
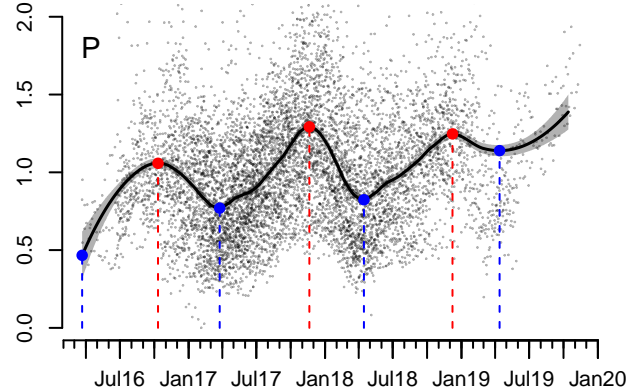
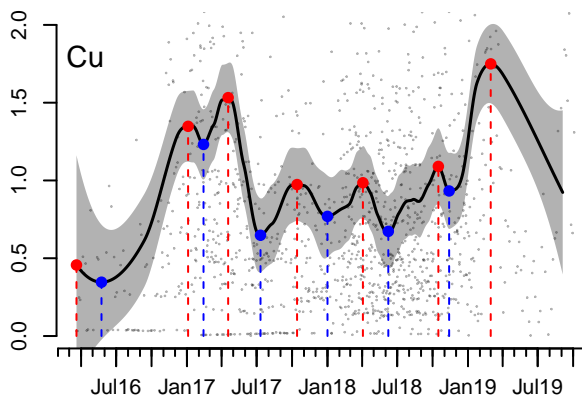
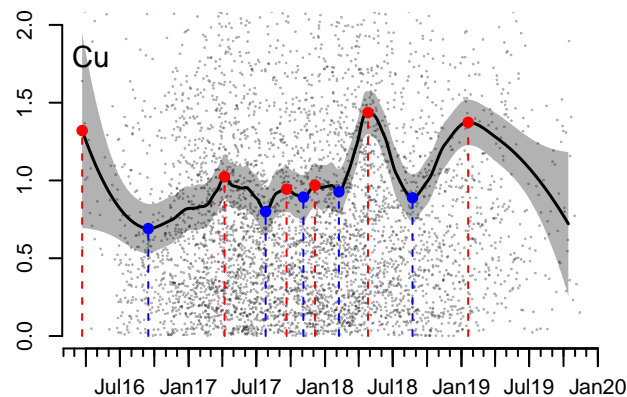








Date



Date